

1 ***DCP2* plays multiple roles during *Drosophila* development – possible case of moonlighting?**

2 Rohit Kumar and Jagat K Roy*

3 Cytogenetics Laboratory, Department of Zoology, Institute of Science, Banaras Hindu University,

4 Varanasi – 221005, Uttar Pradesh, India

5 ***Address for Correspondence –**

6 Jagat K Roy,

7 Cytogenetics Laboratory,

8 Department of Zoology,

9 Institute of Science,

10 Banaras Hindu University,

11 Varanasi – 221005,

12 Uttar Pradesh, India.

13 Fax: +91-542-236-8457

14 E-mail: jkroy@bhu.ac.in

15

16 **Running title – *DCP2* expression in *Drosophila* development**

17

18 ***DCP2* plays multiple roles during *Drosophila* development – possible case of moonlighting?**

19 Rohit Kumar and Jagat K Roy*

20 Cytogenetics Laboratory, Department of Zoology, Institute of Science, Banaras Hindu University,
21 Varanasi – 221005, Uttar Pradesh, India

22 **Abstract**

23 mRNA decapping proteins (DCPs) are components of the P-bodies in the cell which are hubs of mRNAs
24 targeted for decay and they provide the cell with a reversible pool of mRNAs in response to cellular
25 demands. The *Drosophila* genome codes for two decapping proteins, DCP1 and DCP2 out of which
26 DCP2 is the cognate decapping enzyme. The present endeavour explores the endogenous promoter firing,
27 transcript and protein expression of *DCP2* in *Drosophila* wherein, besides a ubiquitous expression across
28 development, we identify active expression paradigm during dorsal closure and a plausible moonlighting
29 expression in the Corazonin neurons of the larval brain. We also demonstrate that the ablation of *DCP2*
30 leads to embryonic lethality and defects in vital morphogenetic processes whereas a knockdown of *DCP2*
31 in the Corazonin neurons reduces the sensitivity to ethanol in adults, thereby ascribing novel regulatory
32 roles to DCP2. Our findings unravel novel putative roles for DCP2 and identify it as a candidate for
33 studies on the regulated interplay of essential molecules during early development in *Drosophila*, nay the
34 living world.

35 **Keywords** – Corazonin/ *DCP2*/ development/ epithelial morphogenesis/ ethanol sedation

36 **Introduction**

37 Organismal development mimics an orchestra with precisely timed and fine-tuned role(s) for each of the
38 players. Balanced expression of genes requires timed activity of gene promoters at the proper site along
39 with orderly degradation of transcripts and/or proteins (Yao and Ndoja, 2012; Ding, 2015). Decay of
40 transcripts is one of the strategies to regulate gene expression (Ghosh and Jacobson, 2010) and the mRNA
41 decapping proteins (DCPs) assume prime importance therein. These proteins initiate degradation of the
42 mRNAs in cytoplasmic foci known as P-bodies, by removal of the 7-methylguanosine cap at the 5' end of
43 the mRNAs (Coller and Parker, 2004). The *Drosophila* genome codes for two mRNA decapping proteins,
44 viz., DCP1 and DCP2, out of which DCP2 is the cognate decapping protein. While DCP1 functions to
45 activate DCP2 (Ren et al, 2012) and P-bodies/DCP1 have been implicated in miRNA mediated gene
46 silencing (Rehwinkel et al, 2005), localization of the oskar mRNA in the *Drosophila* oocyte (Lin et al,
47 2006) and in oogenesis (Lin et al, 2008), DCP2 has been implicated in chronic nicotine induced

48 locomotor hyperactivity in *Drosophila* (Ren et al, 2012). However, characterization of the role of
49 decapping proteins in development has been limited to *Arabidopsis* (Xu et al, 2006) and *Caenorhabditis*
50 *elegans* (Lall et al, 2005) only. Despite being the cognate decapping protein in *Drosophila*, the spatio-
51 temporal dynamics of *DCP2* activity remains unexplored. The gene in *Drosophila* is ~8kb in length, has
52 two curated promoters, viz., a proximal promoter, *DCP2_1* and a second, downstream promoter, *DCP2_2*
53 (Eukaryotic Promoter Database, EPD; Dreos et al, 2014) and codes for four transcripts (FlyBase;
54 Drysdale, 2008). Herein, we have tried to explore the temporal activity of the *DCP2* promoter using the
55 conventional UAS-GAL4 system (Brand and Perrimon, 1993) wherein, we used a GAL4 driven by the
56 *DCP2* promoter (*DCP2^{GAL4}*; Lukacsovich et al, 2001; Ren et al, 2012) and combined it with a modified
57 UAS line (G-TRACE; Evans et al, 2009) to delineate the real-time promoter activity of *DCP2* during
58 embryonic dorsal closure and in the larval tissues. In parallel, we endeavored to delineate the expression
59 of the transcript isoforms or splice variants generated, and the expression paradigm of the translated
60 protein. Although, *DCP2* is highly active and ubiquitous, high expression of the *DCP2* protein was
61 observed in the Corazonin (Crz) neurons of the larval brain and renders the individuals less sensitive to
62 ethanol when knocked down in the corazonin neurons and it is expressed along the A-P and D-V axes in
63 the larval wing pouch. *Loss-of-function* mutants of *DCP2* are embryonic lethal and showed defects in
64 epithelial morphogenesis and organization of the embryonic nervous systems along with elevation and
65 spatial disruption of the JNK cascade. Collectively, our observations present us with a stage for further
66 exploration of hitherto undescribed facets of *DCP2* activity and identify *DCP2* as a potential candidate for
67 explication of molecular interplay during *Drosophila* development.

68 **Materials and Methods**

69 **Fly strains, genetics and lethality assay**

70 All flies were raised on standard agar-cornmeal medium at 24±1°C. *Oregon R⁺* was used as the wild type
71 control. For targeted gene expression (Brand and Perrimon, 1993), *DCP2^{BG01766}/TM3,Ser¹* (*DCP2^{GAL4}* ;
72 Ren et al, 2012), *CCAP-GAL4*, *TH-GAL4*, *Ap-GAL4*, *Ddc-GAL4*, *UAS-GFP*, *UAS-mCD8::GFP* and *UAS-*
73 *DCP2^{RNAi}* were obtained from the Bloomington *Drosophila* Stock Centre, while G-TRACE (Evans et al,
74 2009) was a kind gift from Prof. Utpal Banerjee, MBI, UCLA. *DCP2^{e00034}/TM3, Ser¹* was obtained from
75 the Harvard *Drosophila* Stock Centre. The JNK signaling bio-sensor, *TRE-RFP* (Chatterjee and
76 Bohmann, 2012; referred to as TRE-JNK in the text) was obtained as kind gift from Dr. B. J. Rao, TIFR,
77 Mumbai, India while *sNPF-GAL4*, *Dilp2-GAL4* and *Crz-GAL4/CyO* were procured from Prof. Gaiti
78 Hasan, NCBS, Bangalore, India.

79 *DCP2^{BG01766}/TM3, Ser^l* and *DCP2^{e00034}/TM3, Ser^l* were further introgressed with *TM3, ActGFP,*
80 *Ser^l/TM6B* stock in order to generate *DCP2^{BG01766}/TM3, ActGFP, Ser^l* or *DCP2^{e00034}/TM3, ActGFP, Ser^l*
81 stocks. *TRE-JNK* (Chatterjee and Bohmann, 2012) was introgressed with *Sp/CyO; DCP2^{BG01766}/ TM3,*
82 *ActGFP, Ser^l* or and *Sp/CyO; DCP2^{e00034}/ TM3, ActGFP, Ser^l* to obtain *TRE-JNK; DCP2^{BG01766}/TM3,*
83 *ActGFP, Ser^l* and *TRE-JNK; DCP2^{e00034}/TM3, ActGFP, Ser^l* stocks, respectively.

84 For behaviour assays, *Crz-Gal4/CyO* flies were crossed to *w¹¹¹⁸* or *UAS-DCP2^{RNAi}* flies to generate *Crz-*
85 *Gal4/+* (Control) or *Crz-Gal4/+; UAS-DCP2^{RNAi}/+* (Experimental) genotypes.

86 Embryonic lethality was calculated as described in Bhui and Roy, 2009. 100 embryos were transferred
87 to agar plates and incubated for 24 to 48 h at 23°C and the total number of dead embryos was counted
88 against total number of fertilized eggs. These fertilized eggs include the dead as well as the hatched
89 embryos. The percentage of lethality was calculated as –

90 $(\text{No. of dead embryos}/\text{No. of fertilized embryos}) \times 100\%$

91 The percentage (%) lethality for each cross was calculated in triplicates and the mean lethality so obtained
92 was tabulated and graphically represented using MS-Excel-2010. The final percentages have been
93 calculated by multiplying the lethality obtained in every cross scheme with the inverse of the fraction of
94 the progeny determined by standard Mendelian ratios.

95 **Detection of DCP2 transcript expression and analysis of splice variants**

96 Detection of transcript expression from *DCP2* was performed by reverse-transcriptase polymerase chain
97 reaction (RT-PCR) using a combination of primers designed such that the amplicon size would
98 discriminate between the individual isoforms which included a single reverse primer, *DCP2_DBAE_R,*
99 which could bind to all of the transcripts, and two forward primers, *viz., DCP2_BAE_F* which would bind
100 to isoforms *DCP2-RA, RB* and *RE,* and *DCP2_D_F,* which would bind to *DCP2-RD.* Being similar in
101 architecture, *DCP2-RA* and *RE* would yield similar sized amplicons with the above primer pair, but
102 *DCP2-RD* would yield a smaller amplicon. However, the 3'UTR is longer and unique for *DCP2-RE* and
103 we exploited the architectural bias to discriminate between the two isoforms by designing an additional
104 primer pair which would amplify the 3'UTR sequence of *DCP2-RE* uniquely. The table below (**Table 1**)
105 shows the primer sequences, the combinations and the calculated amplicon sizes for each of the isoform
106 with each of the primer pairs. The unique amplicons are italicized. RT-PCR was performed according to
107 Lakhota et al, 2012 in the samples discussed in the results section.

108 **Table 1:** List of primer sequences, combinations generated and calculated amplicon sizes for detection of
 109 expression of *DCP2* transcript isoforms

Primer Pair	Sequence (5'-3')	Amplicon size (in base pair)			
		RD	RB	RA	RE
DCP2_D_F	ACAACGATTCAATACATATACAGCT	165	-	-	-
DCP2_DBAE_R	CTGTTTTTGTGCTCGTGTGT				
DCP2_BAE_F	GCAATTTAGATCGCGAAAAAGTTC	-	159	974	974
DCP2_DBAE_R	CTGTTTTTGTGCTCGTGTGT				
DCP2_EU_F	TCATTTGTCTGGGCCAAGTGAC	-	-	-	233
DCP2_EU_R	TGGGATTGCAGTTCATCAAATG				

110

111 **Embryo collection and fixation**

112 All flies were made to lay eggs on standard agar plates supplemented with sugar and propanoic acid and
 113 eggs were collected according to Narasimha and Brown, 2006, with slight modifications. For whole
 114 mount preparations and immunostaining of embryos, different alleles and transgenes were balanced with
 115 GFP tagged balancers and only non-GFP or driven embryos were selected for experimental purpose.
 116 Embryo staging was done according to Hartenstein's Atlas of *Drosophila* Development, 1993.

117 **Immunocytochemistry**

118 *Drosophila* embryos were fixed and imaged as described by Narasimha and Brown, 2006. The
 119 dechorionated and devitellized embryos were fixed in 4% para-formaldehyde solution and stored in
 120 absolute methanol. Immunostaining of the embryos was done as described in Nandy and Roy, 2019. Late
 121 third instar larval tissues were dissected out in 1X PBS, fixed in 4% paraformaldehyde for 20 min at RT
 122 and immunostained as described previously in Banerjee and Roy, 2017. The primary antibodies used were
 123 – mouse anti-DCP2 (1:50; PCRP-DCP2-1D6, DSHB), mouse anti-Fasciclin II (1:100; 1D4, DSHB),
 124 mouse anti-Fasciclin III (1:100; 7G10, DSHB) and rabbit anti-phospho-JNK/SAPK (1:100; 81E11 Cell
 125 Signaling Technology). Appropriate secondary antibodies conjugated either with Cy3 (1:200, Sigma-
 126 Aldrich, India) or Alexa Fluor 488 (1:200; Molecular Probes, USA) or Alexa Fluor 546 (1:200; Molecular
 127 Probes, USA) were used to detect the given primary antibody, while chromatin was visualized with DAPI
 128 (4', 6-diamidino-2-phenylindole dihydrochloride, 1µg/ml Sigma-Aldrich). For imaging of live embryos
 129 for real-time promoter analysis using G-TRACE or JNK signaling, embryos of the desired genotype were
 130 rinsed in 1X PBS, dechorionated in bleach and mounted in halocarbon oil and observed directly.

131 **Cuticular preparations from embryos**

132 Cuticle preparations were made from embryos as described by Wieschaus and Nusslein-Volhard, 1986
133 along with some modifications as described in Sasikumar and Roy, 2008. Briefly, the eggs were
134 dechorionated in bleach and washed in an aqueous solution containing 0.7% NaCl and 0.02% Triton-X
135 100. The eggs were washed thrice in 0.1% Triton-X, devitellinised in a mixture of methanol and n-
136 heptane (1:1 v/v) mixture. They were fixed in 1 part glycerol - 4 parts acetic acid for 1 h, mounted in
137 Hoyer's mountant and cleared at 60°C overnight.

138 **Microscopy and Documentation**

139 The immunostained slides were observed under Zeiss LSM 510 Meta Laser Scanning Confocal
140 microscope, analysed with ZEN12 and LSM softwares and assembled using Adobe Photoshop 7.0. The
141 cuticles were observed in dark field or phase-contrast optics, namely 10X Plan Fluor Ph1 DLL (0.3 NA),
142 20X Plan Fluor Ph1 DLL (0.5 NA) and 40X Plan Fluor Ph2 DLL (0.75 NA) objectives (Nikon, Japan)
143 and the images were captured with a Nikon Digital camera DXM1200. Fluorescence imaging of embryos
144 for analysis of *DCP2* promoter using G-TRACE or JNK signaling was done in Nikon 90i Fluorescence
145 microscope under 10X Plan Fluor Ph1 DLL (0.3 NA), 20X Plan Fluor Ph1 DLL (0.5 NA) objectives.

146 **Behaviour Assays**

147 Groups of 20 males and females (1-3 days old) of the desired genotypes, *viz.*, *Crz-Gal4/+* (Control) and
148 *Crz-Gal4/+; UAS-DCP2^{RNAi}/+*, maintained on food vials in a 12L: 12D conditions at 23°C for 1 day were
149 used for the following behaviour assays.

150 **Ethanol Sedation Assay**

151 Ethanol sedation assays were performed as described previously (McClure et al, 2013) with minor
152 alterations. Briefly, flies were transferred to empty vials, sealed with cotton plugs and allowed to
153 acclimatize for 10-20 min. The cotton plugs were replaced with fresh plugs containing 1 ml of 100%
154 ethanol. They were maintained in such “booze chambers” for 15-20 mins. During the treatment, flies were
155 mechanically stimulated by tapping and/or mechanically swirling the vials at intervals of 5 mins. Flies
156 able to climb the walls and/or move their appendages on the floor of the vial were considered “non-
157 sedated” while those unable to execute such activity were considered “sedated”. The number of sedated
158 flies was counted at 5 min intervals. The time to 50% sedation (ST50) was determined by manual
159 extrapolation.

160 **Recovery from Ethanol Sedation**

161 Recovery from ethanol induced sedation was assayed as described by Sha et al, 2014. Following exposure
162 to ethanol (described above), the cotton plugs were replaced with fresh plugs and the vials were inverted
163 to place them upside down. The number of “non-sedated” flies (considered as “recovered”) was counted
164 every 10 min.

165 **Results and Discussion**

166 ***DCP2* mRNAs are expressed ubiquitously throughout *Drosophila* development**

167 In order to determine the presence or absence of *DCP2* at a particular stage alongwith identification of the
168 exact isoform(s)/splice variant(s) expressed therein, RT-PCR was performed using primers designed for
169 the same. *DCP2* expression was detectable at all stages of development, *viz.* embryo (0-24h), larval stages
170 (1st, 2nd and 3rd instars), pupal and adult stages. Among the four annotated variants, *DCP2_RE*
171 (FBtr0304975) and *DCP2_RA* (FBtr0075538) was observed in all stages of fly development, whereas
172 *DCP2_RD* (FBtr0100528) was observed only in the larval gonads, *viz.* testes and ovaries, and in the adult
173 flies (**Figure 1**). The other variant, *DCP2_RB* (FBtr0075539) was detectable only in the pupae and adults
174 but was absent in larval stages. Out of the four isoforms however, *DCP2_RA* and *DCP2_RE* is observed
175 to be expressed throughout development but *DCP2_RE* appears to be the most abundant and ubiquitous
176 isoform expressed. Although, *DCP2-RB* is driven by the same promoter which drives *DCP2_RA* and *RE*,
177 its absence does not necessarily indicate dearth of expression. *In-silico* analyses and data mining from the
178 Eukaryotic Promoter Database (Dreos et al, 2014, 2017) indicate that *DCP2-RD* may be driven by the
179 second promoter of *DCP2* (*DCP2_2*). The protein isoforms coded by *DCP2_RB* and *DCP2_RD* are
180 identical in sequence and size, but the exclusive expression of *DCP2_RD* in the larval gonadal tissues
181 (ovaries and testes) and at a very low titre in the adults may be owing to the promoter being responsive to
182 transcription factors in the gonadal tissues only and/or a putative undiscovered function of the transcript
183 therein, despite absence of visible quantities of *DCP2_RB*.

184 ***DCP2* expresses in cells of diverse developmental lineages in the *Drosophila* embryo and the *DCP2* 185 promoter *vis-à-vis* *DCP2* is active since early development**

186 Evolution has been parsimonious in designing genes and ascribing roles to them and hence, determination
187 of gene functions becomes incomplete without identification of the expression dynamics of the gene. In
188 order to determine the endogenous expression pattern of *DCP2* in *Drosophila melanogaster*, we used the
189 *DCP2^{GAL4}* (*DCP2^{BG01766}*) which has a P{GT1}construct (Lukacsovich et al, 2001) bearing a GAL4,
190 immediately downstream to the *DCP2* promoter. Using GFP as a reporter, we detected extremely robust
191 signal in the late embryonic stages, wherein it expresses strongly in the embryonic epithelia (ectoderm)
192 (**Fig. 2A**), the central nervous system (neuro-ectoderm) (**Fig. 2B**) and the dorsal muscles (mesoderm)

193 **(Fig. 2C)** and is uniformly ubiquitous in all the segments in the embryo. With such a robust expression
194 (of GFP), which is actually driven by the *DCP2* promoter, it is evident that *DCP2* is expressed and is
195 active in embryonic cells derived from differing developmental lineages.

196 Dorsal closure is a major morphogenetic event during embryonic developemnt in *Drosophila* (Martinez-
197 Arias, 1993) and involves an orchestrated interplay of numerous molecules (Lada et al, 2012) to drive the
198 concerted movement of lateral epithelial cell sheets. With *DCP2* being expressed strongly in the
199 embryonic epithelium, we investigated the possibility and nature of activity of the *DCP2* promoter during
200 dorsal closure. To determine the real-time activity of the *DCP2* promoter during dorsal closure, we used a
201 GAL4-responsive tripartite construct, G-TRACE (Evans et al, 2009). Using this transgenic line, in the
202 embryonic stages (**Figure 3**), we observed that *DCP2* expresses in a more or less ubiquitous pattern very
203 early in development, even prior to Stage 10 (**Figure 3A**). However, real-time expression was not
204 detected in Stage 10, in which the germband is fully extended (**Figure 3B and 3D**), and the Stage 12,
205 wherein the germband is fully retracted (**Figure 3J and 3L**). In the intervening stage, wherein the
206 germband starts retracting, *i.e.*, Stage 11, we detect strong expression of *DCP2* (**Figure 3F and 3H**).
207 Again, when the epithelial sweeping initiates following germband retraction (Stage13), we see a surge in
208 the RFP expression (**Figure 3N and 3P**) which intensifies further in Stage 14, in which the lateral
209 epithelia on either side are still moving (**Figure 3R and 3T**). This intense RFP expression is visible in
210 Stage 16 as well (**Figure 3V and 3X**). The Stages 10 and 12 are developmental periods of low cell
211 migration as against Stages 11, 13 and 14 wherein the epithelium moves as an initiative of collective cell
212 migration and coordinated cell-shape changes. The expression potential of the *DCP2* promoter across DC
213 revealed expression “crests and troughs”, such that the “crests” paralleled the periods in which cellular
214 mobility or migration was maximal and *vice-versa* (**Figure 3Y**). The RFP activity is detectable only in
215 stages which involve collective cell movement. The eGFP expression however depicts an early initial
216 pulse of the gene expression which plausibly maintains a basal level of gene product. Hence, the
217 dynamics of the promoter reflects a tightly regulated expression of *DCP2* and brings to light that *DCP2*
218 may be an essential player during collective cell migration *vis-à-vis* epithelial morphogenesis.

219 ***DCP2* expresses in the amnioserosa and lateral epithelium during dorsal closure and its loss affects** 220 **survival, epithelial morphogenesis and development of nervous system in the *Drosophila* embryo**

221 Since *DCP2* shows active expression paradigms during embryonic dorsal closure (**Figure 9**), we
222 examined the expression of *DCP2* in the lateral epithelia in Stage 13 embryos along with the expression
223 of activated JNK, a key mediator of dorsal closure (Jacinto et al, 2002), and Fasciclin III, a cell adhesion
224 molecule (Bahri et al, 2010), both of which are expressed at the lateral epithelia and the leading edge (LE)

225 cells. DCP2 was found to be expressed in the amnioserosa and throughout the lateral epithelium as well as
226 in the cells at the LE (**Figure 4**). During the later stages of dorsal closure, parallel to the contra-lateral
227 movement of the epithelia towards the dorsal side, the axon pathways are pioneered in the CNS across the
228 ventral nerve cord, which form the complete nervous system by the end of Stage 16 (Bhuin and Roy,
229 2009). Examination of the ventral nerve cord also showed strong cytoplasmic expression of DCP2
230 (**Figure 5**).

231 We found that embryos homozygous for loss-of-function alleles of *DCP2* (*viz.*, *DCP2^{BG01766}* and
232 *DCP2^{e00034}*) show embryonic lethality. *DCP2^{BG01766}* homozygotes are 100% embryonic lethal (N=500)
233 whereas *DCP2^{e00034}* homozygotes show 12% lethality (N=500) at the embryonic stage and the remaining
234 die before reaching the second instar larval stage.

235 **Defects in Epithelial Morphogenesis**

236 Since we found strong expression of *DCP2* in the embryonic epithelium, we endeavored to explore
237 whether a loss of *DCP2* function affects epithelial morphogenesis. Analysis of embryonic cuticles showed
238 that all mutants displayed pronounced defects in epithelial morphogenesis patterns, ranging from defects
239 in size, *viz.*, antero-posterior or dorso-ventral dimensions, head involution defects and morphological
240 defects, *viz.*, u-shaped or puckering (**Figures 6**). Since these defects are not mutually exclusive in that, a
241 single mutant embryo could be displaying multiple defects at the same time, the morphological
242 aberrations were scored individually first and then analysed for the presence of other concomitant defects.
243 While 82.6% of the *DCP2^{BG01766}* homozygotes show altered antero-posterior or dorso-ventral dimensions
244 (*viz.*, elongated or compressed) of which 68.4% embryos are defective in head involution and 36.8%
245 embryos are puckered, 21.7% embryos have gross defects in all the morphological parameters analysed.
246 4.3% of the embryos are exclusively puckered and 6.5% embryos show defects in head involution only.
247 None of the *DCP2^{e00034}* homozygotes analysed was exclusively puckered. 80% of the embryos observed
248 show altered dimensions out of which 12.5% are puckered and are defective in head involution and 62.5%
249 embryos are not puckered but show head involution defects. 20% of the embryos observed show defects
250 exclusively in dimensions or head involution. Figure 7 shows the above data represented with the help of
251 a Venn diagram.

252 **Defects in Nervous System development**

253 We used mAbBP102, an antibody to mark all CNS axons (Seeger et al. 1993) such that the gross
254 morphology of CNS in an embryo is revealed. In wild-type embryos, axons form an orthogonal structure
255 having longitudinal axon tracts. These axon tracts run antero-posteriorly, being positioned at either side

256 of the midline, and a pair of commissural tracts joins the longitudinal pathways in each segment of the
257 embryo (Bhuin and Roy, 2009). *DCP2*^{BG01766} homozygotes showed thinning of longitudinal connectives
258 and compressed segmental commissures (**Figure 8 B and B'**) similar to the *karussell* phenotype
259 (Hummel et al, 1999), whereas, *DCP2*^{e00034} homozygotes showed thinning of longitudinal connectives
260 and lateral commissures (**Figure 8 C and C'**).

261 In order to study the embryonic PNS axons further, mutant embryos were stained with mAb22C10, which
262 recognizes the microtubule-associated protein, futsch (Hummel et al. 2000). It labels all the cell bodies,
263 dendrites, and axons of all PNS neurons, and a subset of neurons in the VNC of the CNS (Fujita et al.
264 1982). Therefore, defects, such as the disruption of the nervous system, the collapse of the axon tracts,
265 fasciculation defects/thinning of axons, and the loss or gain of neurons can often be distinguished. In the
266 wild type embryos, each segment contains three highly stereotyped clusters of PNS neurons connected by
267 axon bundles. In the mutants, misrouting of axons and collapsed axons could be detected (**Fig. 8 E, E'**
268 **and F, F'**), which were absent in the wild type, implying a role for DCP2 in the fasciculating axons.

269 ***DCP2* loss-of-function mutants show elevation and spatial perturbation of JNK signaling**

270 The JNK signaling cascade is an essential player of *Drosophila* gastrulation *vis-à-vis* embryonic
271 development wherein it modulates important events such as dorsal closure (Jacinto et al, 2002; Kushnir et
272 al., 2017) and architecture of the nervous systems (Shklover et al, 2015; Karkali et al, 2016). Since *DCP2*
273 *loss-of-function* mutants show defects associated with either process, we wanted to investigate the spatial
274 expression of the JNK cascade. We harnessed the bio-sensor, TRE-RFP to identify the spatial pattern of
275 JNK signaling (Chatterjee and Bohmann, 2012) in the wild type embryos and in embryos homozygous for
276 *loss-of-function* alleles of *DCP2*. Both *DCP2*^{BG01766} and *DCP2*^{e00034} homozygotes showed enhanced RFP
277 expression, implying an elevation in the JNK signaling cascade. Further, the pattern of RFP *vis-à-vis* JNK
278 signaling is spatially disrupted in the *DCP2* mutants, implying a perturbation and/or misregulated JNK
279 signaling (**Figure 9**). In the wild type embryos it is expressed at the juncture of the two epithelial sheets
280 following completion of dorsal closure, mimicking the stitch at a suture, whereas the mutant homozygotes
281 show a spatial distortion of JNK signaling.

282 In the developing *Drosophila* embryo undergoing gastrulation, epithelial morphogenesis and
283 axonogenesis are morphogenetic events of utmost importance that require a well orchestrated spatio-
284 temporal regulation of gene expression. During initiation of dorsal closure wherein the two lateral
285 epithelia initiate contra-lateral movement to eventually seal the dorsal opening, the dorsal-most lateral
286 epithelial cells express high levels of JNK (Noselli and Agnes, 1999). The JNK signaling pathway is a
287 core signaling pathway in the process of dorsal closure at the time of gastrulation in *Drosophila* embryos

288 (Noselli, 1998; Noselli and Agnes, 1999; Ramet et al 2002; Stronach and Perrimon, 2002). While *DCP2*
289 co-expresses with JNK ubiquitously on the dorso-lateral epithelia, the leading edge and the amnioserosa,
290 monitoring the activity of the *DCP2* promoter in real time across the stages of dorsal closure shows spurts
291 of promoter firing in the stages which involve large scale cell migration and movement. Such subtle and
292 precisely timed gene activity is indicative of thorough fine-tuning of the expression of *DCP2*. The
293 ablation of *DCP2* does not lead to “dorsal open” embryos, but generates a spectrum of defects including
294 altered embryonic dimensions and defects in head involution, improper fasciculation of axons and defects
295 in segmental commissures and longitudinal connectives, causes embryonic and larval lethality implies
296 significant perturbation in these developmental gene expression programs and indicate a more concerted
297 and fundamental role of *DCP2* in regulating these phenomena. It is worth mentioning that despite
298 ubiquitous expression of *DCP2*, the ectodermal (epithelium) and neuro-ectodermal (CNS and PNS)
299 tissues are most affected following ablation. It is interesting to note that while the nematode worm is a
300 closer relative of the fly in the evolutionary tree, the embryonic lethality and the developmental defects
301 are similar to those observed in a distant relative, *Arabidopsis* (Xu et al, 2006; Goeres et al, 2007). Since
302 the JNK signaling pathway is fundamental to the process of dorsal closure during gastrulation in
303 *Drosophila* embryos (Noselli, 1998; Noselli and Agnes, 1999; Ramet et al, 2002; Stronach and Perrimon,
304 2002) and both epithelial morphogenesis and CNS development are dependent on JNK activity (Jacinto et
305 al, 2002; Kushnir et al., 2017; Shklover et al, 2015; Karkali et al, 2016), the altered expression patterns of
306 JNK or misdirected JNK signaling under the influence of loss of *DCP2* in the different alleles could be a
307 probable cause of the defects observed in each case.

308 **The *DCP2* promoter shows consistent developmental activity in the larval tissues along with tissue-** 309 **specific expression paradigms of the translated protein**

310 Real-time activity of the promoter in the various larval tissues, with a better insight, demonstrates that
311 despite expression since early development, the *DCP2* promoter is active during late stages of larval
312 development as well. In the larval tissues (118±1 h ALH), we could identify a consistent GFP expression
313 in the larval brain, eye-antennal disc, salivary gland and wing discs. Besides prior developmental
314 activation and ubiquitous expression, the *DCP2* promoter shows enhanced activity/expression in specific
315 cells in the brain (**Figure 10 B and C**) and eye disc (**Figure 10 G and H**). Although, the ventral ganglion
316 depicts an overlap of prior and real-time activity (**Figure 10 B-D**), the cerebral hemispheres show
317 selective expression in real-time, which is limited to cells of the antennal lobe and the Kenyon cells
318 (**Figure 10 B'-D'**). Similarly, the cells in constituting the antennal disc show a more consistent *DCP2*
319 activity, exemplified the greater degree of overlap of the reporters (**Figure 10 G-I**). However, the cells of
320 the eye disc show heterogeneity of reporter expression, *viz.*, *DCP2* is active in all the ommatidia but

321 certain cells show a transient activity at the stage observed (**Figure 10 G'-I'**). While the salivary gland
322 nuclei show a complete colocalization of reporters with similar intensity (**Figure 10 L-N**), wing discs
323 show a lower expression of eGFP as compared to RFP.

324 Since, the GAL4 is driven by the *de novo* promoter of *DCP2*, which in absence of the GAL4 coding
325 region, would have transcribed the gene *per se*, this transgenic construct, *viz.*, G-TRACE allows the
326 spatio-temporal expression potential of the promoter to be determined. Thus, the expression of the
327 reporters (GFP and RFP) may be directly correlated with the gene expression pattern or potential in the
328 wild type individual and hence, *via* the GAL4, directly demonstrates the spatio-temporal gene expression
329 dynamics.

330 **Brain**

331 In the larval brain, immunolocalisation of DCP2 shows a uniform cytoplasmic expression throughout the
332 dorso-ventral and antero-posterior axes of the tissue (**Figure 11A', B' and D'**). However, significantly
333 high levels were detected in a subset of neurons in the ventral ganglion (**Figure 11A' and D'**) and in a
334 cluster of neurons in the dorso-lateral and dorso-medial region of the central brain (**Figure 11A' and C'**),
335 which are proximal to the Mushroom Body as well as in the Kenyon cells (**Figure 11K and O**).
336 However, it is completely absent from the most prominent neuronal structures *viz.*, the Mushroom Body
337 in the central brain and in the neurons of the optic lobe (**Figure 11M-O**).

338 **Salivary Glands**

339 In the salivary glands, DCP2 shows a punctuate distribution in the cytoplasm and decorates the nuclear
340 and cellular membranes arduously (**Figure 11E' and E''**). The cytoplasmic vesicles appear bounded by
341 bodies rich in DCP2 (**Figure 11E''**). Since DCP2 is a cognate resident of the P-bodies, it may be fair
342 enough to interpret the cytoplasmic network of DCP2 punctae in the glands as the pattern of P-bodies
343 which are essential for maintaining transcript homoeostasis.

344 **Wing discs**

345 The wing discs show very strong expression of DCP2 in the pouch region as compared with the notum
346 (**Figure 11F'**), besides the uniform ubiquitous cytoplasmic distribution similar to that observed in other
347 tissues. Most notably, the expression of DCP2 in the central sections of the pouch overlaps with the
348 expression of the Antero-Posterior determinant Decapentaplegic (Dpp) (Zecca et al, 1995) and the
349 Dorso-Ventral determinant Wingless (Wg) (Neumann and Cohen, 1997), thereby presenting a

350 “cruciform” pattern in the pouch (**Figure 11G**), which may be essential during the morphogenesis of the
351 wing blade.

352 Immunolocalisation of DCP2 to the cytoplasm in all the tissues examined across development
353 recapitulates the results observed in similar studies in the nematode worm, *C. elegans* (Lall et al, 2005)
354 and in the thale cress, *Arabidopsis* (Xu et al, 2006). In spite of uniform ubiquitous cytoplasmic expression
355 in the larval tissues, certain paradigms of expression have been noticed. The protein shows distinct
356 punctate expression of the protein in the wing imaginal disc along the antero-posterior and dorso-ventral
357 axes in the wing pouch, mimics the expression patterns of the TGF-beta homologue Decapentaplegic and
358 Wingless, respectively. In the salivary glands as well, the protein is cytoplasmic but shows high titres at
359 the membranes. Being the sole decapping agent in *Drosophila*, DCP2 is expressed ubiquitously
360 throughout development but, the selectively high expression in certain cell types in the brain or the wing
361 pouch point towards some yet unknown “moonlighting” functions of *DCP2* in the development and
362 maintenance of cellular homeostasis in these tissues.

363 **DCP2 shows high expression in the Corazonin neurons in the larval CNS**

364 Besides ubiquitous expression, DCP2 has a typical expression paradigm in a subset of neurons in the
365 larval CNS. In order to identify/type the DCP2 immunopositive neuron(s) in the larval ventral nerve cord
366 (VNC), we tried mapping them against the Fasciclin II (FasII) landmark system (Santos et al, 2007)
367 (**Figure 12**). Comparing the FasII “coordinates” with the DCP2 expression paradigm, we observed that
368 DCP2 expresses in a cluster of three neurons in the Dorso-lateral (DL) region and in a neuron located
369 medial to the DL neurons (Dorso-medial; DM) in the central brain, and in eight pairs of bilateral neurons
370 in the ventral nerve cord. The neurons in the ventral ganglion correspond to a subset of the thoracic (T2
371 and T3) and abdominal (A1 – A6) neuromeres. Although DCP2 is absent from the most prominent
372 neuronal structures expressing FasII, *viz.*, the Mushroom Body and the neurons innervating the eye, in the
373 central brain (**Figure 12 D-F**) and in the Dorso-lateral and Dorso-medial longitudinal tracts in the VNC
374 (**Figure 12 G-I**), the DL neurons appear to innervate the Ring gland and the aorta. Lateral views of the
375 central brain (**Figure 12 D'-F'**) and the VNC (**Figure 12 G'-I'**) show that the DCP2-positive neurons lie
376 below the Fas II immunopositive Dorso-lateral and Dorso-medial longitudinal tracts but ascend above the
377 Mushroom Body (MB) in the central brain.

378 While DCP2 did not show co-expression with the different neuropeptides *viz.* Crustacean Cardioactive
379 Peptide (CCAP; Veverlytsa and Allan, 2012), *Drosophila* Insulin like Peptide-2 (Dilp2; Liu et al, 2016),
380 Corazonin (Crz; Lee et al, 2008) and short Neuropeptide F (sNPF; Nassel et al, 2008), biogenic amines
381 Tryptophan hydroxylase (TH; Friggi-Grelin et al, 2003) and Dopamine decarboxylase (Ddc; Vomel and

382 Wegener, 2008), or the transcription factor Apterous (Ap; Rincon-Limas et al, 1999) (**Supplementary**
383 **Figure 2**), complete colocalization or overlap of expression was observed with the neurons expressing
384 Corazonin (**Figure 13**), while only the Dorso-lateral neurons showed co-expression with sNPF
385 (**Supplementary Figure 3**). Corazonin neurons constitute three neuronal subsets, *viz.*, the dorso-lateral
386 (DL) and dorso-medial Crz neurons (DM), and the Crz neurons in the ventral nerve cord (vCrz) (Lee et al,
387 2008), are essential for combating stress (Zhao et al, 2010) and co-express the transcription factor
388 Apontic, which is necessary and sufficient to mediate sensitivity to ethanol (McClure, 2013).

389 **Knockdown of *DCP2* in the Corazonin neurons reduces sensitivity to Ethanol**

390 We further asked whether *DCP2* function in the Corazonin neurons is required for their activity. When
391 *DCP2* was knocked down in these neurons specifically, it did not affect the morphology, pathfinding or
392 architecture of the Crz neurons in the larval brain (**Supplementary Figure 4**) but, delayed and/or reduced
393 the sedation sensitivity to ethanol in the adult flies. The time to 50% sedation (ST50) was calculated to be
394 ~8.5 min for the control flies (N=200), while the *DCP2* knocked down flies showed an ST50 of ~13.5
395 min (N=200). While the control flies are sedated completely in ~12 min, the *DCP2* hypomorphs are
396 active till ~19 min (**Figure 14 A and B**). This demonstrates the reduced sensitivity of the *Crz GAL4>UAS*
397 *DCP2* RNAi knocked down flies to ethanol.

398 Following sedation, the *DCP2* hypomorphs showed early onset of recovery (~30 min) as against the
399 control flies, which started showing activity/onset of recovery after ~110 min. While the control flies
400 started assuming normal standing posture in ~2h, the *DCP2* knocked down flies showed significant early
401 recovery, with ~80% of the flies recovering by 3h as against ~40% recovery exhibited by the control flies
402 in the same time (**Figure 14 C and D**). Also, sedation induced death was higher in the control group as
403 compared to the *DCP2* hypomorphs. During sedation and recovery phases, no sex specific differences
404 were observed in flies of either genotype. These results suggest that *DCP2* function is required in the Crz
405 neurons for regulation of ethanol related behaviour and ethanol metabolism.

406 The Crz neurons require the transcription factor Dimmed and its target enzyme, Peptidylglycine-alpha-
407 hydroxylating monooxygenase (PHM) (Park et al, 2008) for synthesis of Corazonin while the
408 transcription factor Apontic (Apt) is necessary and sufficient for regulating the activity of the Crz neurons
409 and/or release of Corazonin during ethanol exposure (McClure, 2013). The delay in sedatory behaviour
410 during ethanol exposure and the quick recovery from sedation demonstrate impaired function of the Crz
411 neurons and/or perturbed corazonin signaling following knockdown of *DCP2* in the Crz neurons,
412 although the mechanism behind such altered physiology remains unknown.

413 **Summary and Conclusion**

414 Analysis and identification of the expression patterns of genes and/or proteins in model organisms across
415 the evolutionary tree are important for understanding the spectral paradigm of gene function. The extent
416 to which a gene and its expressome are conserved across diverse organisms indicates the precision of its
417 function across phyla. mRNA decapping proteins are present in all metazoans and serve to initiate the
418 decay of mRNA and are therefore important for regulation of gene expression *vis-à-vis* cellular
419 physiology. The patterns of expression and paradigm range of physiological aberrations following the
420 ablation or knockdown of *DCP2* is indicative of the fundamental regulatory role played by it during
421 development and bring to light the hitherto undiscovered plausible novel functions of *DCP2*. It is yet
422 unknown as to whether it's function in the modulation of developmental events is *via* the *de novo*
423 function of mRNA decapping or is a manifestation of moonlighting behaviour (Mani et al, 2014) .
424 Summarizing the present observations, our findings demonstrate that *DCP2* plays a major modulatory
425 function in developmental gene expression and is essential for maintenance of organismal physiology at
426 all stages of development.

427

428 **Acknowledgements**

429 The authors acknowledge the fly community for generously providing fly stocks. We thank Prof. B. J.
430 Rao, TIFR, Mumbai for providing the *TRE-JNK/CyO* stock, Prof. Gaiti Hasan, NCBS, Bangalore for
431 providing the *sNPF-GAL4*, *Dilp2-GAL4* and *Crz-GAL4/CyO* stocks and Prof. Utpal Banerjee, UCLA for
432 providing the *G-TRACE/CyO* flies. We duly acknowledge the National Facility for Laser Scanning
433 Confocal Microscopy, Department of Zoology, Banaras Hindu University. Financial support from DST-
434 FIST, UGC-UPE and CAS Zoology are duly acknowledged. We sincerely acknowledge Nabarun Nandy
435 for assistance, valuable discussions and proofreading the manuscript. We sincerely thank Department of
436 Science and Technology (DST) for providing INSPIRE Fellowship to RK.

437

438 **Author Contributions**

439 RK, conceptualization, resources, methodology, investigation, data curation, formal analysis and
440 interpretation, writing the manuscript. JKR, supervision, resources, analysis and interpretation, writing the
441 manuscript.

442 **Conflict of Interest**

443 The authors declare no conflict of interest.

444

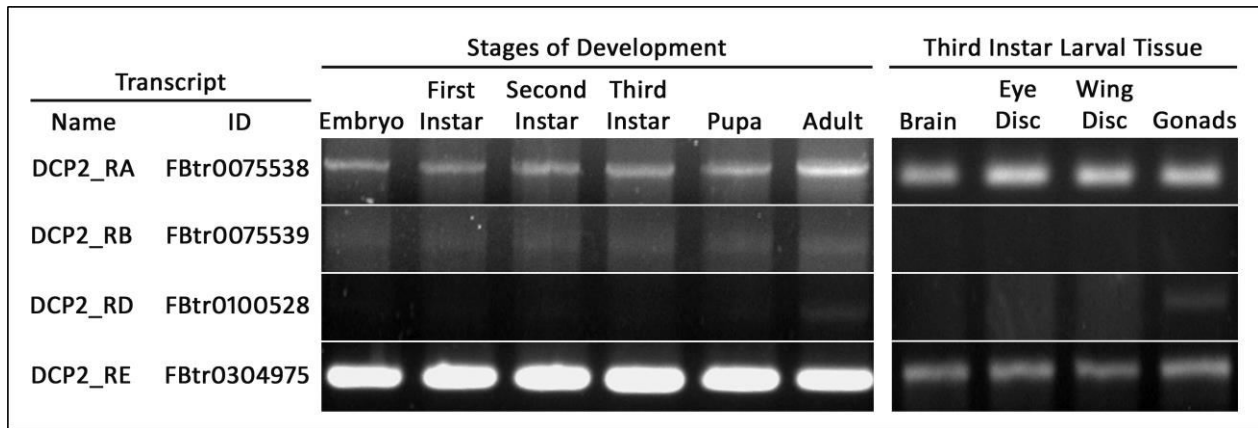
445 **References**

- 446 Bahri, S., Wang, S., Conder, R., Choy, J., Vlachos, S., Dong, K., Merino, C., Sigrist, S., Molnar, C., Yang,
447 X. and Manser, E., 2010. The leading edge during dorsal closure as a model for epithelial plasticity: Pak is
448 required for recruitment of the Scribble complex and septate junction formation. *Development*, 137(12),
449 pp.2023-2032.
- 450 Banerjee, A. and Roy, J.K., 2017. Dicer-1 regulates proliferative potential of *Drosophila* larval neural stem
451 cells through bantam miRNA based down-regulation of the G1/S inhibitor Dacapo. *Developmental*
452 *biology*, 423(1), pp.57-65.
- 453 Baojin, D.I.N.G., 2015. Gene expression in maturing neurons: regulatory mechanisms and related
454 neurodevelopmental disorders. *Acta Physiologica Sinica*, 67(2), pp.113-133.
- 455 Bhui, T. and Roy, J.K., 2009. Rab11 is required for embryonic nervous system development in
456 *Drosophila*. *Cell and tissue research*, 335(2), pp.349-356.
- 457 Brand, A.H. and Perrimon, N., 1993. Targeted gene expression as a means of altering cell fates and
458 generating dominant phenotypes. *Development*, 118(2), pp.401-415.
- 459 Chatterjee, N. and Bohmann, D., 2012. A versatile Φ C31 based reporter system for measuring AP-1 and
460 Nrf2 signaling in *Drosophila* and in tissue culture. *PLoS one*, 7(4), p.e34063.
- 461 Collier, J. and Parker, R., 2004. Eukaryotic mRNA decapping. *Annual review of biochemistry*, 73(1),
462 pp.861-890.
- 463 Dreos, R., Ambrosini, G., Groux, R., Cavin Périer, R. and Bucher, P., 2016. The eukaryotic promoter
464 database in its 30th year: focus on non-vertebrate organisms. *Nucleic acids research*, 45(D1), pp.D51-D55.
- 465 Dreos, R., Ambrosini, G., Périer, R.C. and Bucher, P., 2014. The Eukaryotic Promoter Database:
466 expansion of EPDnew and new promoter analysis tools. *Nucleic acids research*, 43(D1), pp.D92-D96.
- 467 Drysdale, R. and FlyBase Consortium, 2008. FlyBase. In *Drosophila* (pp. 45-59). Humana Press.
- 468 Evans, C.J., Olson, J.M., Ngo, K.T., Kim, E., Lee, N.E., Kuoy, E., Patananan, A.N., Sitz, D., Tran, P., Do,
469 M.T. and Yackle, K., 2009. G-TRACE: rapid Gal4-based cell lineage analysis in *Drosophila*. *Nature*
470 *methods*, 6(8), p.603.
- 471 Friggi-Grelin, F., Coulom, H., Meller, M., Gomez, D., Hirsh, J. and Birman, S., 2003. Targeted gene
472 expression in *Drosophila* dopaminergic cells using regulatory sequences from tyrosine hydroxylase.
473 *Journal of neurobiology*, 54(4), pp.618-627.
- 474 Fujita, S.C., Zipursky, S.L., Benzer, S., Ferrus, A. and Shotwell, S.L., 1982. Monoclonal antibodies against
475 the *Drosophila* nervous system. *Proceedings of the National Academy of Sciences*, 79(24), pp.7929-7933.
- 476 Ghosh, S. and Jacobson, A., 2010. RNA decay modulates gene expression and controls its fidelity. *Wiley*
477 *Interdisciplinary Reviews: RNA*, 1(3), pp.351-361.

- 478 Goeres, D.C., Van Norman, J.M., Zhang, W., Fauver, N.A., Spencer, M.L. and Sieburth, L.E., 2007.
479 Components of the Arabidopsis mRNA decapping complex are required for early seedling
480 development. *The Plant Cell*, 19(5), pp.1549-1564.
- 481 Hartenstein, V., 1993. *Atlas of Drosophila development* (Vol. 328). Cold Spring Harbor Laboratory Press.
- 482 Hummel, T., Krukkert, K., Roos, J., Davis, G. and Klämbt, C., 2000. *Drosophila* Futsch/22C10 is a
483 MAP1B-like protein required for dendritic and axonal development. *Neuron*, 26(2), pp.357-370.
- 484 Jacinto, A., Woolner, S. and Martin, P., 2002. Dynamic analysis of dorsal closure in *Drosophila*: from
485 genetics to cell biology. *Developmental cell*, 3(1), pp.9-19.
- 486 Karkali, K., Panayotou, G., Saunders, T.E. and Martin-Blanco, E., 2016. The JNK signaling links the CNS
487 architectural organization to motor coordination in the *Drosophila* embryo.
- 488 Kushnir, T., Mezuman, S., Bar-Cohen, S., Lange, R., Paroush, Z.E. and Helman, A., 2017. Novel interplay
489 between JNK and Egfr signaling in *Drosophila* dorsal closure. *PLoS genetics*, 13(6), p.e1006860.
- 490 Lada, K., Gorfinkiel, N. and Arias, A.M., 2012. Interactions between the amnioserosa and the epidermis
491 revealed by the function of the u-shaped gene. *Biology open*, 1(4), pp.353-361.
- 492 Lakhotia, S.C., Mallik, M., Singh, A.K. and Ray, M., 2012. The large noncoding hsr ω -n transcripts are
493 essential for thermotolerance and remobilization of hnRNPs, HP1 and RNA polymerase II during recovery
494 from heat shock in *Drosophila*. *Chromosoma*, 121(1), pp.49-70.
- 495 Lall, S., Piano, F. and Davis, R.E., 2005. *Caenorhabditis elegans* decapping proteins: localization and
496 functional analysis of Dcp1, Dcp2, and DcpS during embryogenesis. *Molecular biology of the cell*, 16(12),
497 pp.5880-5890.
- 498 Lee, G., Kim, K.M., Kikuno, K., Wang, Z., Choi, Y.J. and Park, J.H., 2008. Developmental regulation and
499 functions of the expression of the neuropeptide corazonin in *Drosophila melanogaster*. *Cell and tissue*
500 *research*, 331(3), pp.659-673.
- 501 Lin, M.D., Fan, S.J., Hsu, W.S. and Chou, T.B., 2006. *Drosophila* decapping protein 1, dDcp1, is a
502 component of the oskar mRNP complex and directs its posterior localization in the oocyte. *Developmental*
503 *cell*, 10(5), pp.601-613.
- 504 Lin, M.D., Jiao, X., Grima, D., Newbury, S.F., Kiledjian, M. and Chou, T.B., 2008. *Drosophila* processing
505 bodies in oogenesis. *Developmental biology*, 322(2), pp.276-288.
- 506 Liu, Y., Liao, S., Veenstra, J.A. and Nässel, D.R., 2016. *Drosophila* insulin-like peptide 1 (DILP1) is
507 transiently expressed during non-feeding stages and reproductive dormancy. *Scientific reports*, 6, p.26620.
- 508 Lukacsovich, T., Asztalos, Z., Awano, W., Baba, K., Kondo, S., Niwa, S. and Yamamoto, D., 2001. Dual-
509 tagging gene trap of novel genes in *Drosophila melanogaster*. *Genetics*, 157(2), pp.727-742.
- 510 Mani, M., Chen, C., Amblee, V., Liu, H., Mathur, T., Zwicke, G., Zabad, S., Patel, B., Thakkar, J. and
511 Jeffery, C.J., 2014. MoonProt: a database for proteins that are known to moonlight. *Nucleic acids research*,
512 43(D1), pp.D277-D282.

- 513 Martinez Arias, A., 1993. Development and patterning of the larval epidermis of *Drosophila*. *The*
514 *development of Drosophila melanogaster*, 1, pp.517-608.
- 515 McClure, K.D. and Heberlein, U., 2013. A small group of neurosecretory cells expressing the
516 transcriptional regulator apontic and the neuropeptide corazonin mediate ethanol sedation in
517 *Drosophila*. *Journal of Neuroscience*, 33(9), pp.4044-4054.
- 518 Nandy, N. and Roy, J.K., 2019. Rab11 is essential for lgl mediated JNK–Dpp signaling in dorsal closure
519 and epithelial morphogenesis in *Drosophila*. *bioRxiv*, p.713115.
- 520 Narasimha, M. and Brown, N.H., 2006. Confocal Microscopy of *Drosophila* Embryos. In *Cell*
521 *Biology* (pp. 77-86). Academic Press.
- 522 Nässel, D.R., Enell, L.E., Santos, J.G., Wegener, C. and Johard, H.A., 2008. A large population of diverse
523 neurons in the *Drosophila* central nervous system expresses short neuropeptide F, suggesting multiple
524 distributed peptide functions. *BMC neuroscience*, 9(1), p.90.
- 525 Neumann, C.J. and Cohen, S.M., 1997. Long-range action of Wingless organizes the dorsal-ventral axis of
526 the *Drosophila* wing. *Development*, 124(4), pp.871-880.
- 527 Noselli, S. and Agnès, F., 1999. Roles of the JNK signaling pathway in *Drosophila*
528 morphogenesis. *Current opinion in genetics & development*, 9(4), pp.466-472.
- 529 Noselli, S., 1998. JNK signaling and morphogenesis in *Drosophila*. *Trends in Genetics*, 14(1), pp.33-38.
- 530 Park, D., Veenstra, J.A., Park, J.H. and Taghert, P.H., 2008. Mapping peptidergic cells in *Drosophila*:
531 where DIMM fits in. *PloS one*, 3(3), p.e1896.
- 532 Rämetsch, M., Lanot, R., Zachary, D. and Manfrulli, P., 2002. JNK signaling pathway is required for
533 efficient wound healing in *Drosophila*. *Developmental biology*, 241(1), pp.145-156.
- 534 Rehwinkel, J.A.N., Behm-Ansmant, I., Gatfield, D. and Izaurralde, E., 2005. A crucial role for GW182
535 and the DCP1: DCP2 decapping complex in miRNA-mediated gene silencing. *Rna*, 11(11), pp.1640-1647.
- 536 Ren, J., Sun, J., Zhang, Y., Liu, T., Ren, Q., Li, Y. and Guo, A., 2012. Down-regulation of Decapping
537 Protein 2 mediates chronic nicotine exposure-induced locomotor hyperactivity in *Drosophila*. *PloS*
538 *one*, 7(12), p.e52521.
- 539 Rincón-Limas, D.E., Lu, C.H., Canal, I., Calleja, M., Rodríguez-Esteban, C., Izpisua-Belmonte, J.C. and
540 Botas, J., 1999. Conservation of the expression and function of apterous orthologs in *Drosophila* and
541 mammals. *Proceedings of the National Academy of Sciences*, 96(5), pp.2165-2170.
- 542 Santos, J.G., Vömel, M., Struck, R., Homberg, U., Nässel, D.R. and Wegener, C., 2007. Neuroarchitecture
543 of peptidergic systems in the larval ventral ganglion of *Drosophila melanogaster*. *PLoS One*, 2(8), p.e695.
- 544 Sasikumar, S. and Roy, J.K., 2009. Developmental expression of Rab11, a small GTP-binding protein in
545 *Drosophila* epithelia. *Genesis*, 47(1), pp.32-39.

- 546 Seeger, M., Tear, G., Ferres-Marco, D. and Goodman, C.S., 1993. Mutations affecting growth cone
547 guidance in *Drosophila*: genes necessary for guidance toward or away from the midline. *Neuron*, 10(3),
548 pp.409-426.
- 549 Sha, K., Choi, S.H., Im, J., Lee, G.G., Loeffler, F. and Park, J.H., 2014. Regulation of ethanol-related
550 behavior and ethanol metabolism by the Corazonin neurons and Corazonin receptor in *Drosophila*
551 melanogaster. *PLoS One*, 9(1), p.e87062.
- 552 Shklover, J., Mishnaevski, K., Levy-Adam, F. and Kurant, E., 2016. JNK pathway activation is able to
553 synchronize neuronal death and glial phagocytosis in *Drosophila*. *Cell death & disease*, 6(2), p.e1649.
- 554 Stronach, B. and Perrimon, N., 2002. Activation of the JNK pathway during dorsal closure in *Drosophila*
555 requires the mixed lineage kinase, slipper. *Genes & development*, 16(3), pp.377-387.
- 556 Veverytsa, L. and Allan, D.W., 2012. Temporally tuned neuronal differentiation supports the functional
557 remodeling of a neuronal network in *Drosophila*. *Proceedings of the National Academy of Sciences*,
558 109(13), pp.E748-E756.
- 559 Vömel, M. and Wegener, C., 2008. Neuroarchitecture of aminergic systems in the larval ventral ganglion
560 of *Drosophila melanogaster*. *PLoS One*, 3(3), p.e1848.
- 561 Wieschaus, E. and Nüsslein-Volhard, C., 1986. *Drosophila: A practical approach*. IRL Press, Oxford,
562 England, p.200.
- 563 Xu, J., Yang, J.Y., Niu, Q.W. and Chua, N.H., 2006. Arabidopsis DCP2, DCP1, and VARICOSE form a
564 decapping complex required for postembryonic development. *The Plant Cell*, 18(12), pp.3386-3398.
- 565 Yao, T. and Ndoja, A., 2012, July. Regulation of gene expression by the ubiquitin-proteasome system.
566 In *Seminars in cell & developmental biology* (Vol. 23, No. 5, pp. 523-529). Academic Press.
- 567 Zecca, M., Basler, K. and Struhl, G., 1995. Sequential organizing activities of engrailed, hedgehog and
568 decapentaplegic in the *Drosophila* wing. *Development*, 121(8), pp.2265-2278.
- 569 Zhao, Y., Bretz, C.A., Hawksworth, S.A., Hirsh, J. and Johnson, E.C., 2010. Corazonin neurons function
570 in sexually dimorphic circuitry that shape behavioral responses to stress in *Drosophila*. *PLoS One*, 5(2),
571 p.e9141.

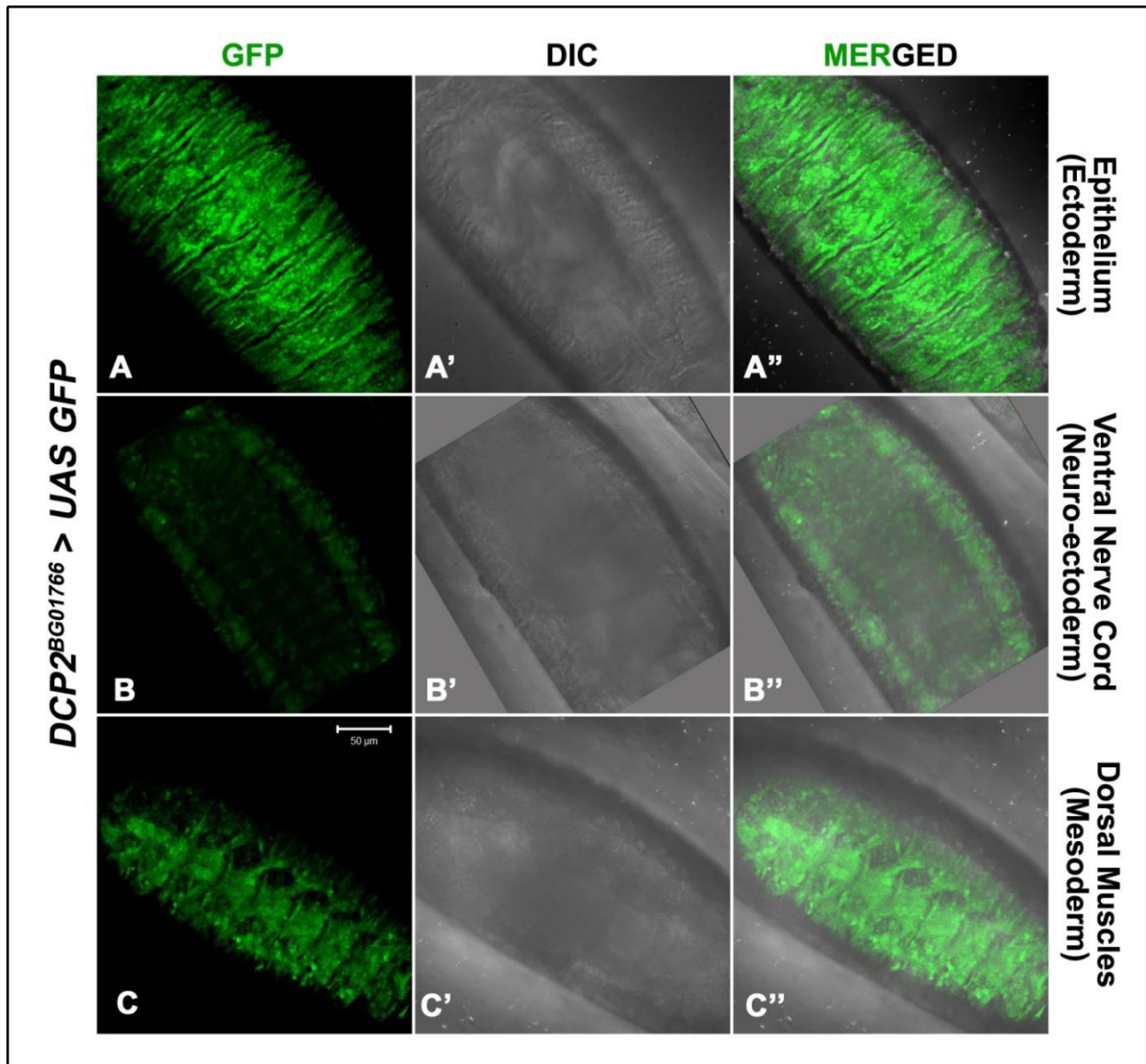


1

2 **Figure 1:** Electrophoretogram showing the expression pattern of different isoforms or splice variants of
3 *DCP2* across *Drosophila* development and in selected third instar larval tissues.

4

5

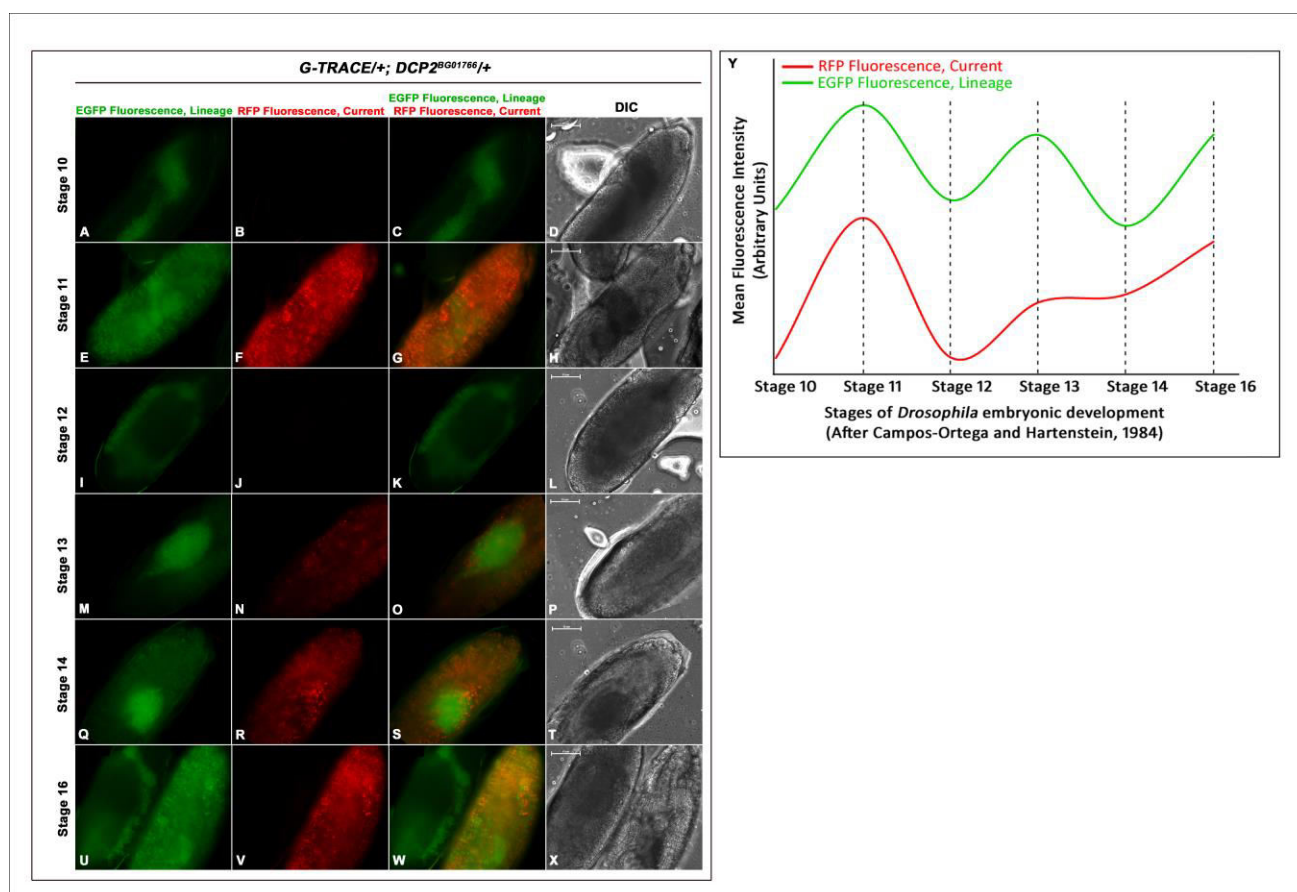


6

7 **Figure 2:** Confocal projections of late embryos (Stage 17) showing endogenous expression pattern of
8 *DCP2* as determined by expression of GFP (green) by *DCP2*^{GAL4}. Tissues of differing developmental
9 lineages, viz., ectoderm (A-A''), neuro-ectoderm (B-B'') and mesoderm (C-C'') show robust expression of
10 GFP.

11

12

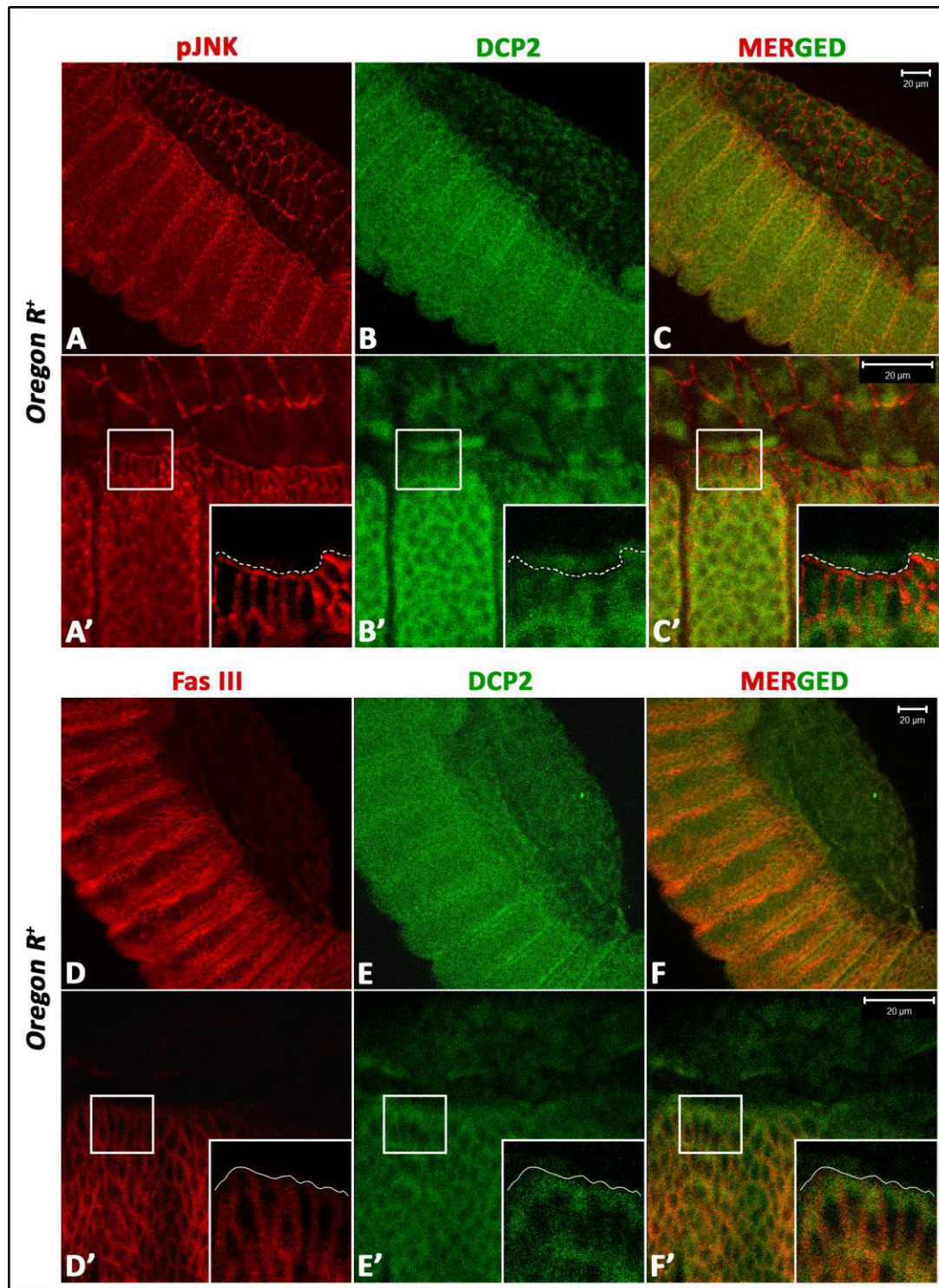


13

14 **Figure 3:** Lineage specific (EGFP) and real time (RFP) expression of *DCP2* in the embryonic stages
15 using the GAL4-UAS based G-TRACE system. A-X show the expression pattern of the reporters along
16 with the DIC images of the embryos. While real-time *DCP2* promoter activity is not detectable during
17 Stages 10 and 12 and is low in Stage 13, it is robust in Stages 11 and 14. Y shows a plot of the
18 fluorescence of both the reporters (GFP and RFP) across the stages observed, wherein a near-sinusoidal
19 curve is obtained showing crests and troughs of *DCP2* promoter activity across the stages of Dorsal
20 closure.

21

22

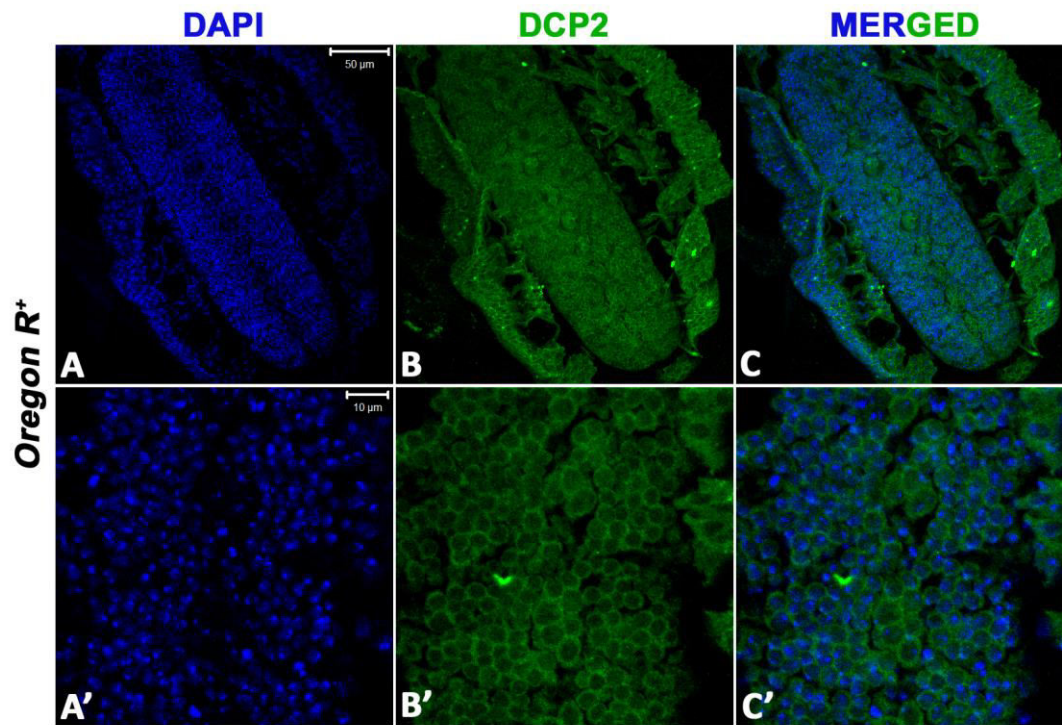


23

24 **Figure 4:** Confocal projections showing immunolocalisation of DCP2 in the amnioserosa and the lateral
25 epithelium in Stage 13 embryos of wild type strain, co-stained for phospho-JNK (A-C) or the septate
26 junction marker FasIII (D-F). In both cases, punctate expression of DCP2 in the lateral epithelium and

27 amnioserosa (B and E) and at the leading edge (B' and E') is clearly visible.

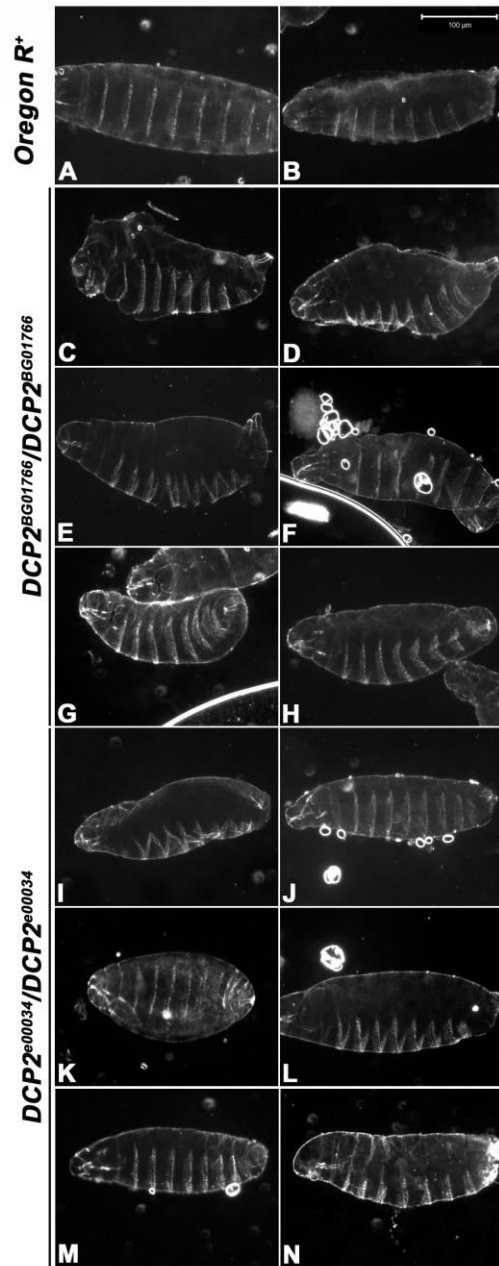
28



29

30 **Figure 5:** Confocal projections showing immunolocalisation of DCP2 in the ventral nerve cord of Stage
31 16 embryos of wild type strain show cytoplasmic expression of DCP2 (B and B') in the ventral nerve
32 cord. Nuclei are counterstained with DAPI.

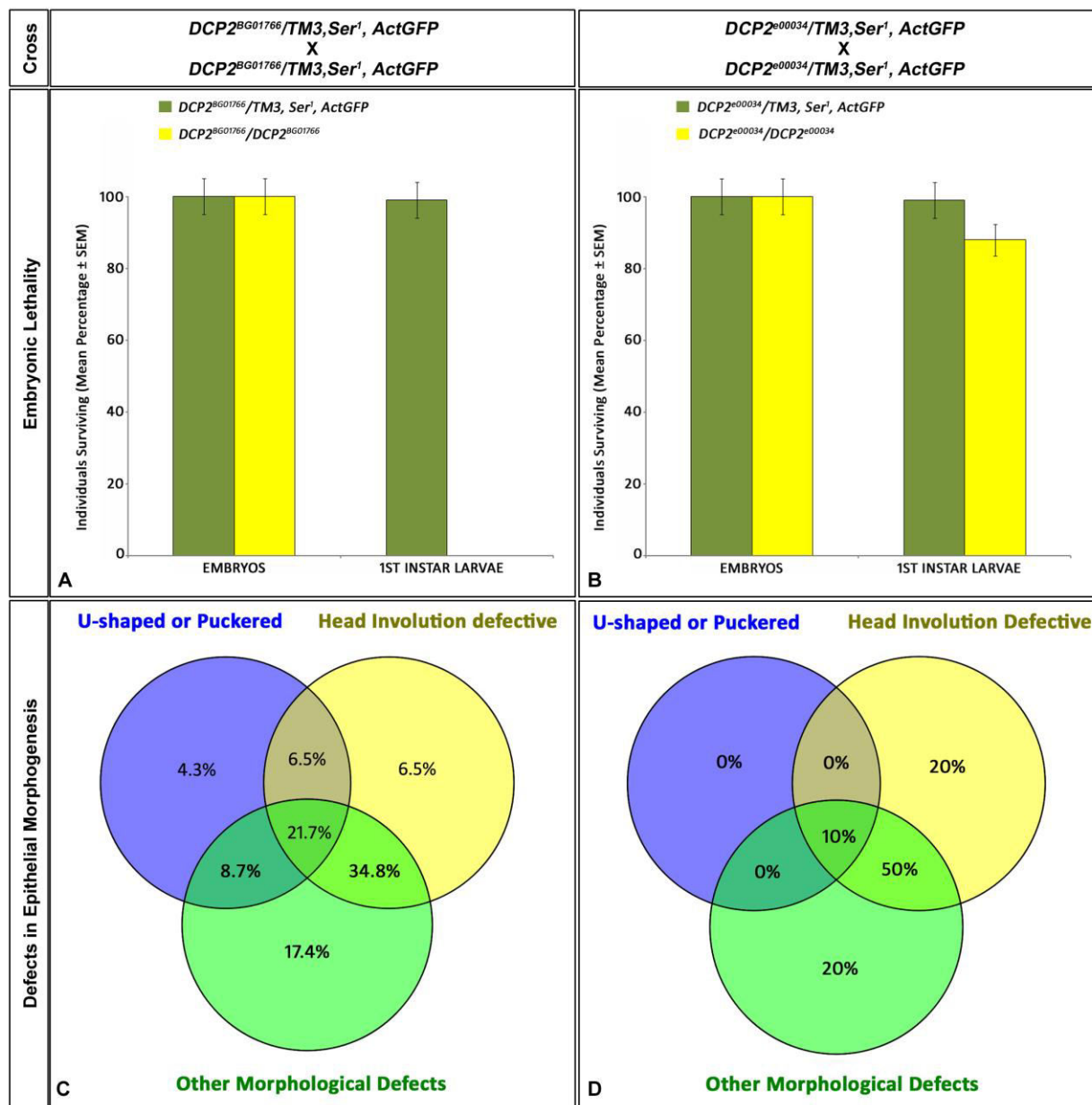
33



34

35 **Figure 6:** Dark field photomicrographs of embryonic cuticles of the wild type (A and B) and $DCP2$ loss-
36 of-function homozygotes, viz., $DCP2^{BG01766}$ (C – H) and $DCP2^{e00034}$ (I – N). Note the altered dimensions
37 and /or morphology and defects in head involution exhibited by the mutants as compared to the wild type.

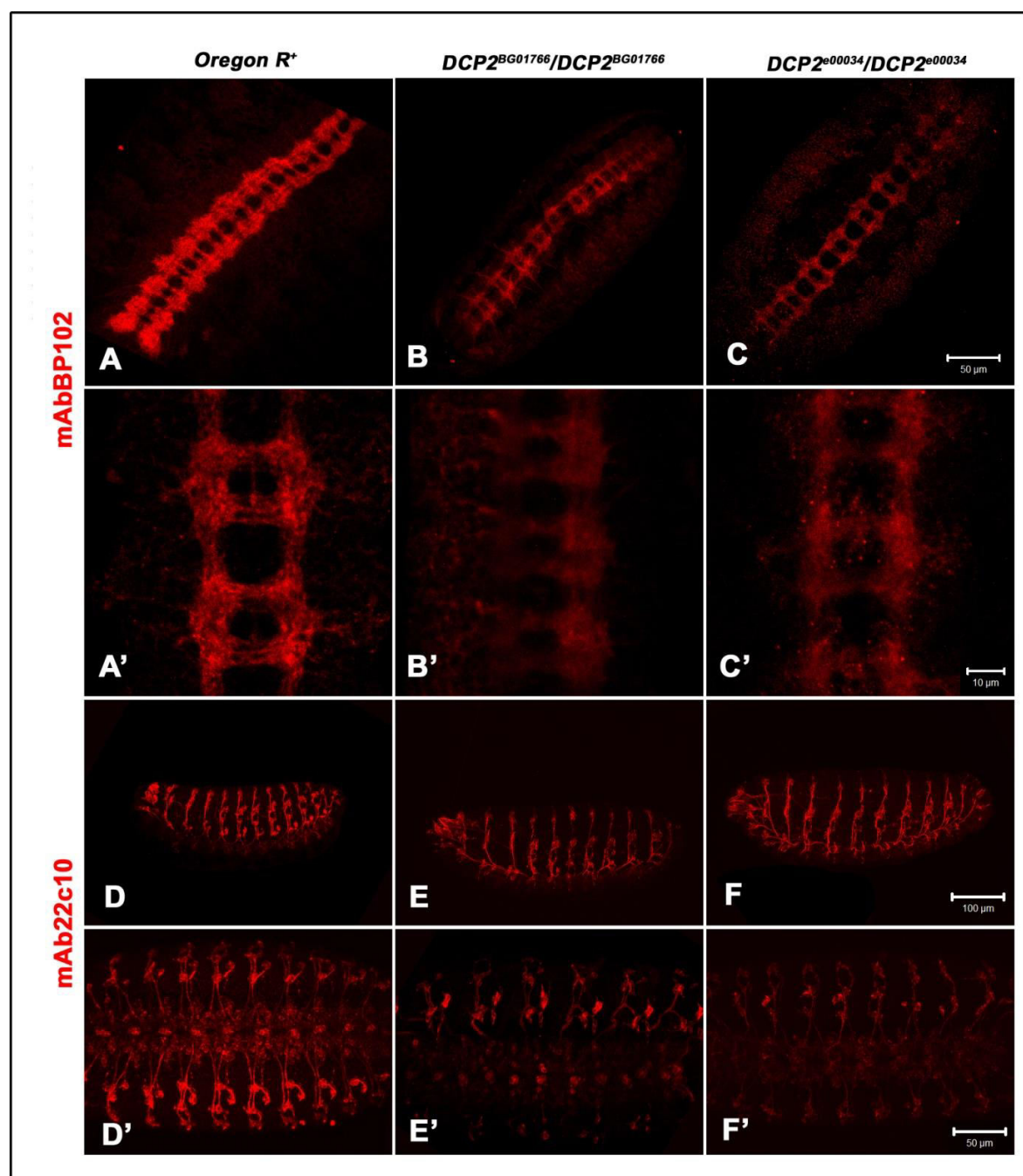
38



39

40 **Figure 7:** Embryonic Lethality and Defects in Epithelial Morphogenesis in *DCP2* loss-of-function
41 homozygotes. *DCP2^{BG01766}* homozygotes are 100% embryonic lethal (A) and exhibit a broader range of
42 epithelial morphogenesis defects being altered in antero-posterior or dorso-ventral dimensions along with
43 puckering and defective head involution (C), but *DCP2^{e00034}* homozygotes show only 12% lethality at the
44 embryonic stage and display a milder range of defects with none of them being exclusively u-shaped or
45 puckered (B).

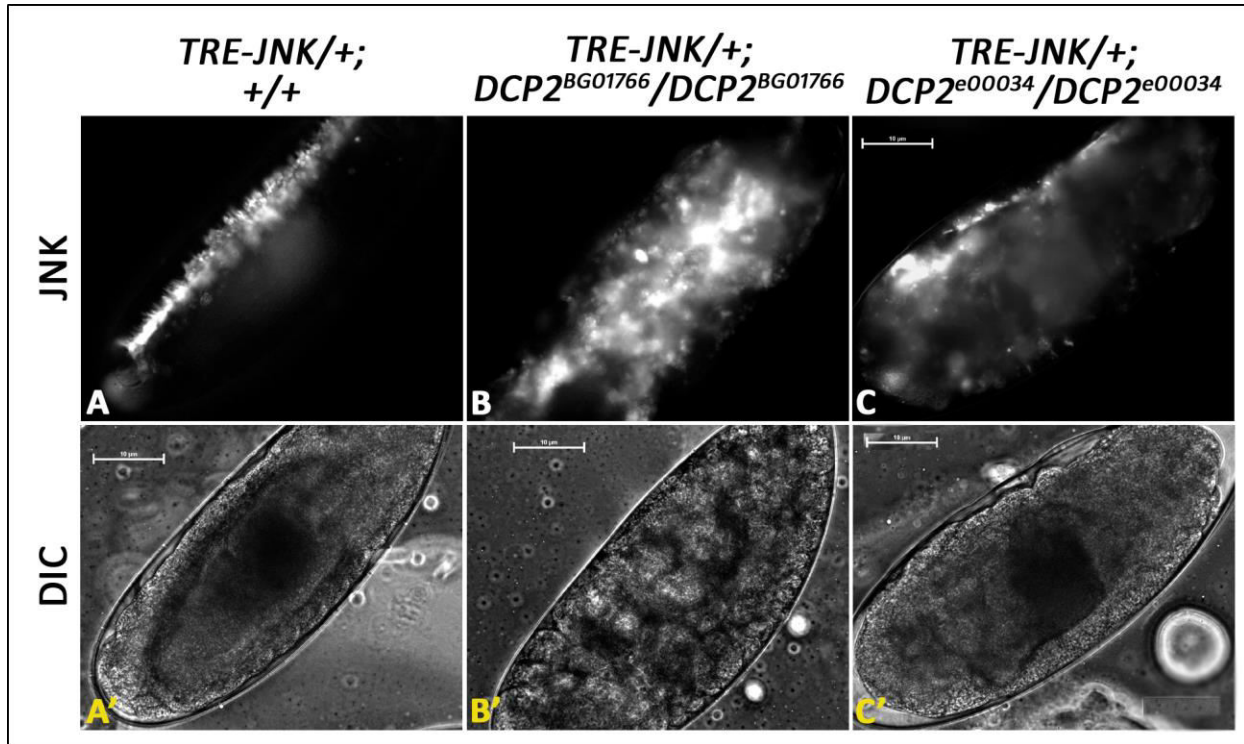
46



47

48 **Figure 8:** *DCP2* null homozygotes display defects in CNS and PNS organization. Upper panel: Wild type
49 embryos, stained with mAbBP102 show regular arrangement of longitudinal connectives and segmental
50 commissures (A and A'). *DCP2*^{BG01766} homozygotes showed thinning of longitudinal connectives and
51 compressed segmental commissures (B and B'), whereas *DCP2*^{e00034} homozygotes showed thinning of
52 longitudinal connectives and lateral commissures (C and C'). Lower panel: In the PNS, axons run from
53 the ventral nerve cord to the periphery of the embryos in each hemisegment (D and D'). A loss of *DCP2*
54 causes misrouting and collapse of fasciculating axons (E and E'; F and F').

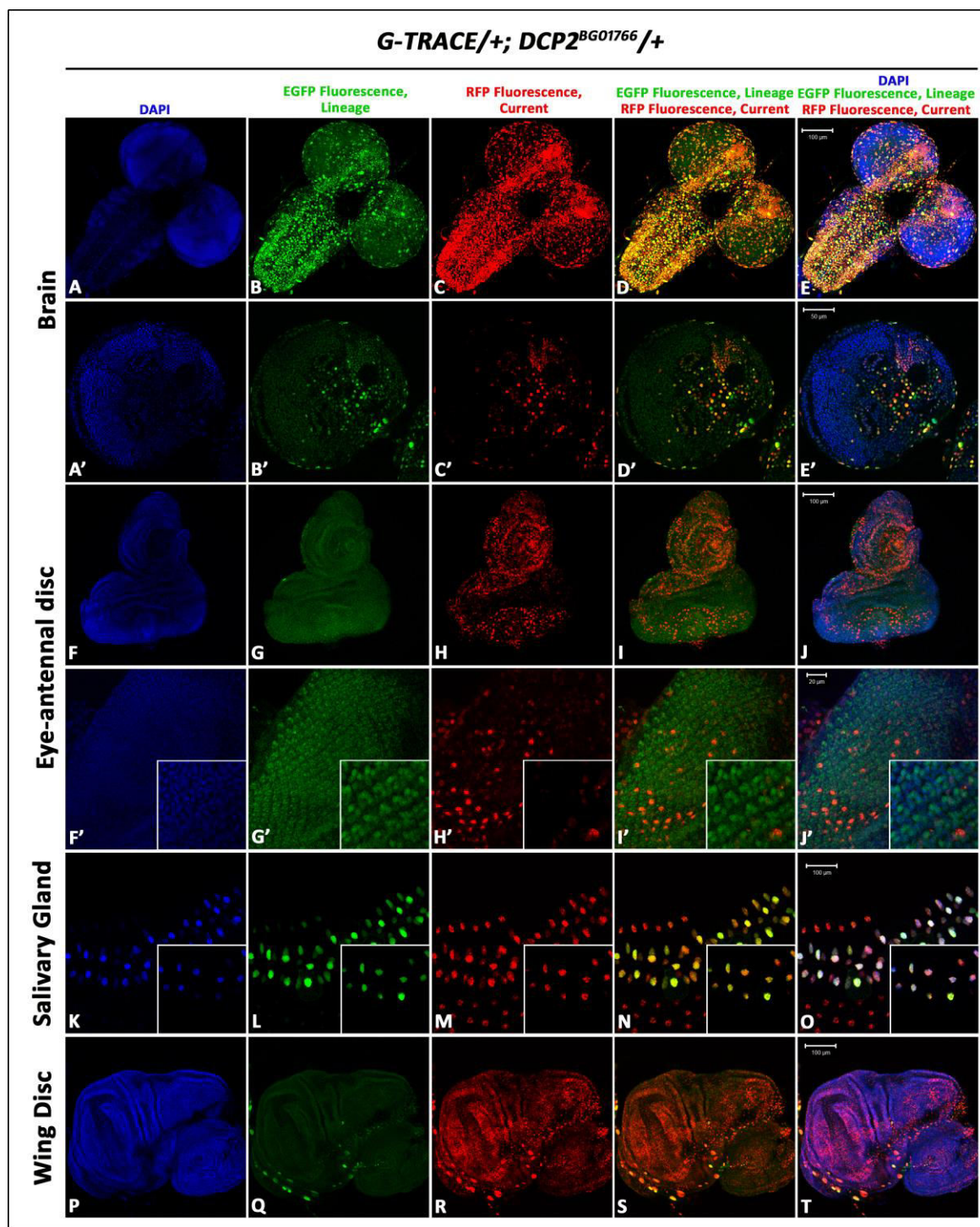
55



56

57 **Figure 9:** Expression of JNK as determined by the biosensor, TRE-JNK in Stage 15 embryos of wild type
58 and *DCP2* loss-of-function mutants. While JNK appears as a suture in the wild type embryos (A and A'),
59 it's spatial expression is completely disrupted in *DCP2* mutant homozygotes (B and C).

60

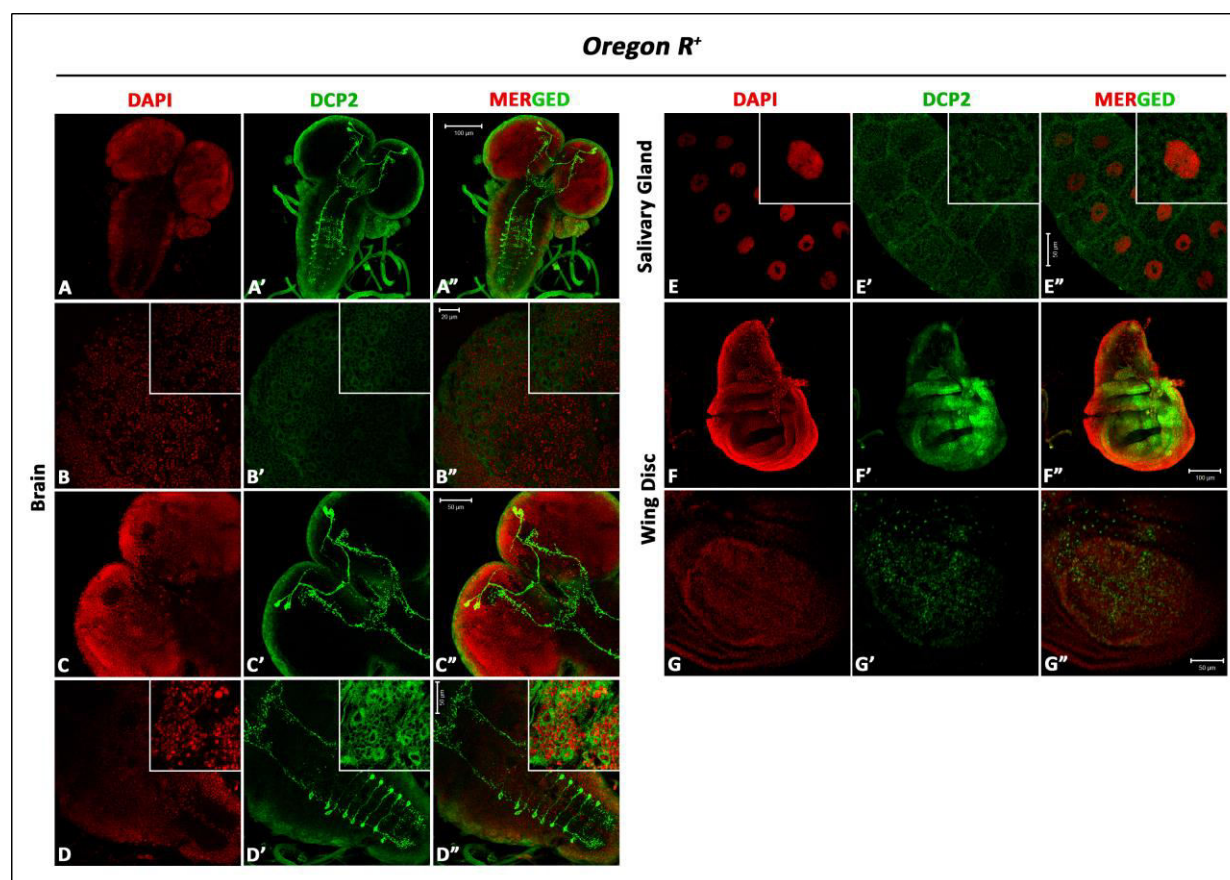


61

62 **Figure 10:** Lineage specific (EGFP) and real time (RFP) expression of *DCP2* in the larval tissues using
63 the GAL4-UAS based *G-TRACE* system. Although the ventral ganglion (B and C) and the antennal disc
64 (G and H) show significant overlap of the reporters, the central brain (B' and C') and the eye-disc (G' and
65 H') show heterogeneity of expression. The salivary gland nuclei and the wing disc show strong real-time

66 expression of the *DCP2* promoter alongwith prior developmental expression.

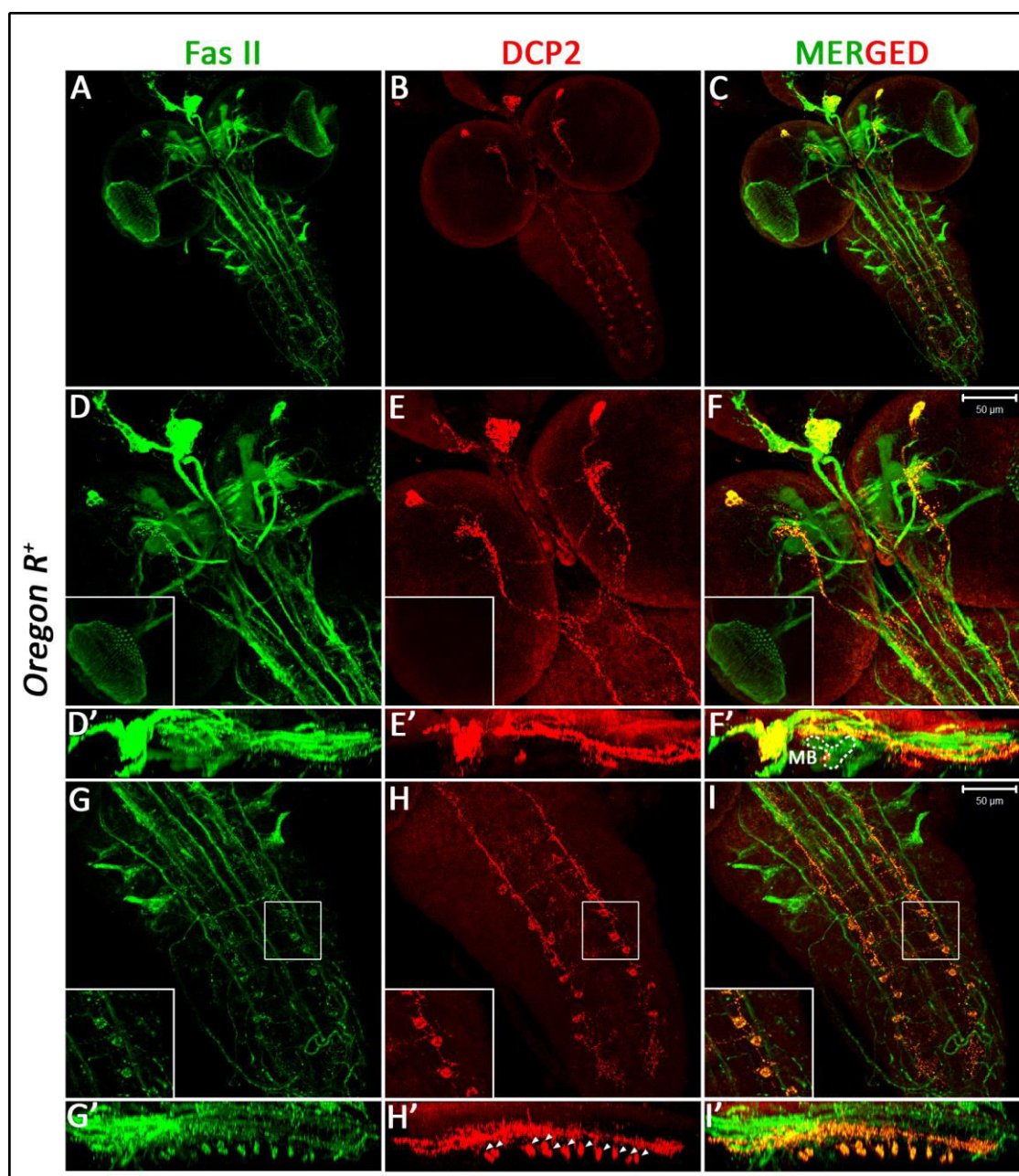
67



68

69 **Figure 11:** Confocal projections showing immunolocalisation of DCP2 in the larval tissues. A-A'' shows
70 the expression pattern in the larval brain. B, C and D show higher magnifications of the same, wherein we
71 find a ubiquitous cytoplasmic expression of DCP2. Visible in C' and D' are a subset of neurons which
72 show high expression of DCP2. In the salivary glands (E), besides cytoplasmic expression, the vesicles in
73 the cytoplasm appear to be arduously decorated with punctate distribution of DCP2. F shows the pattern
74 of expression of DCP2 in the wing disc. Shown in G is a confocal section which shows a magnified view
75 of the wing pouch wherein DCP2 at the antero-posterior and dorso-ventral margins in a cruciform
76 pattern.

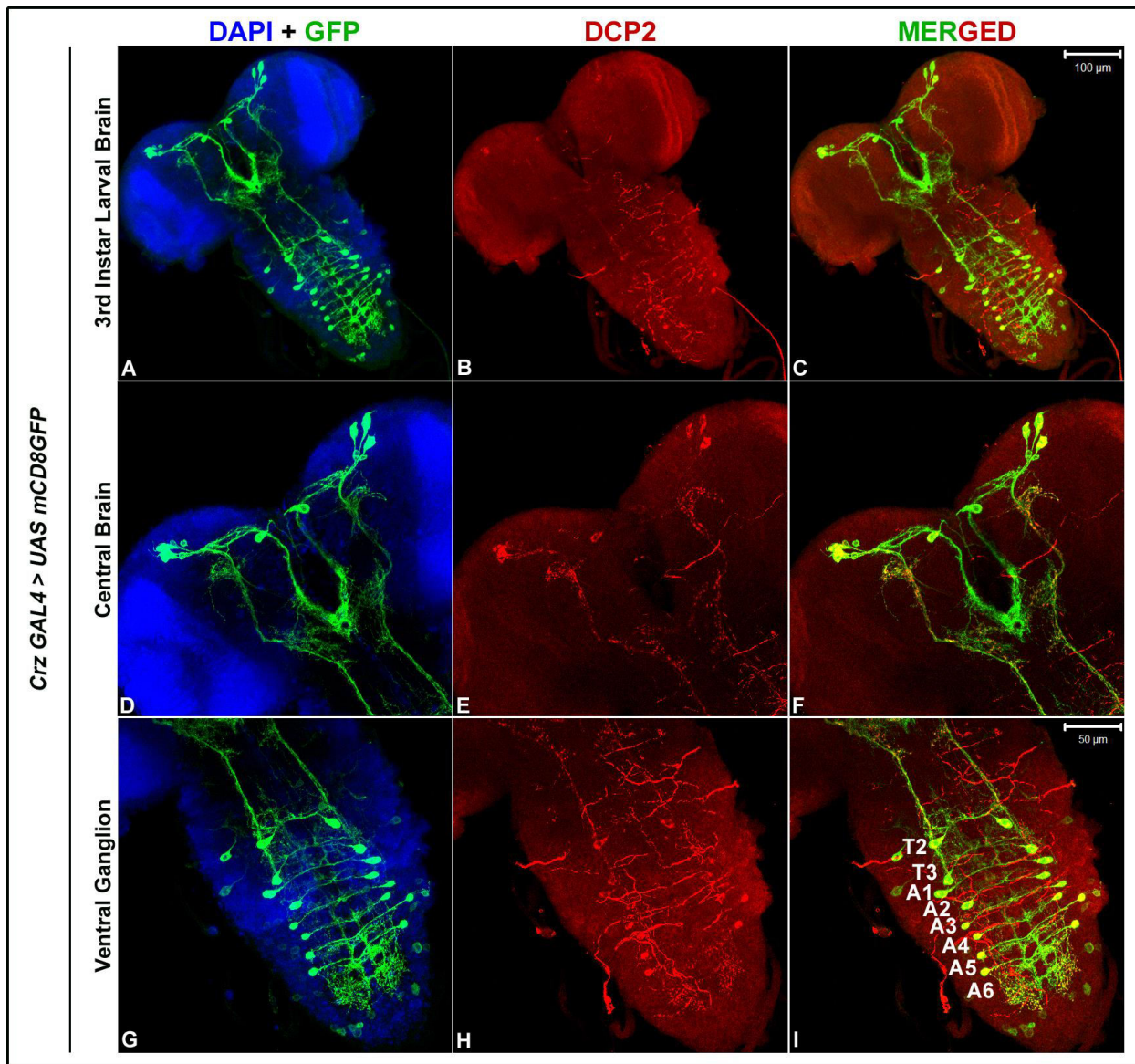
77



78

79 **Figure 12:** Mapping of the neuron(s) expressing high titres of DCP2 in the whole mount preparations of
80 the larval brain (A-C) in the FasII landmark system (Santos et al, 2007). Note the absence of DCP2 in the
81 neurons of the optic lobe (inset D-F). Z-axis stacks show that the DCP2 positive immunopositive
82 neuronal tracts lie below the FasII immunopositive tracts in the larval ventral ganglion but ascend over
83 the Mushroom Body (MB) in the central brain (D'-F'). However, a subset of thoracic and abdominal
84 neuromeres co-express FasII and DCP2 (G-I). Z-axis stacks (G' – I') showing lateral view of the larval
85 ventral ganglion depicted in G-I demonstrate co-expression of FasII and DCP2 in the neuromeres.

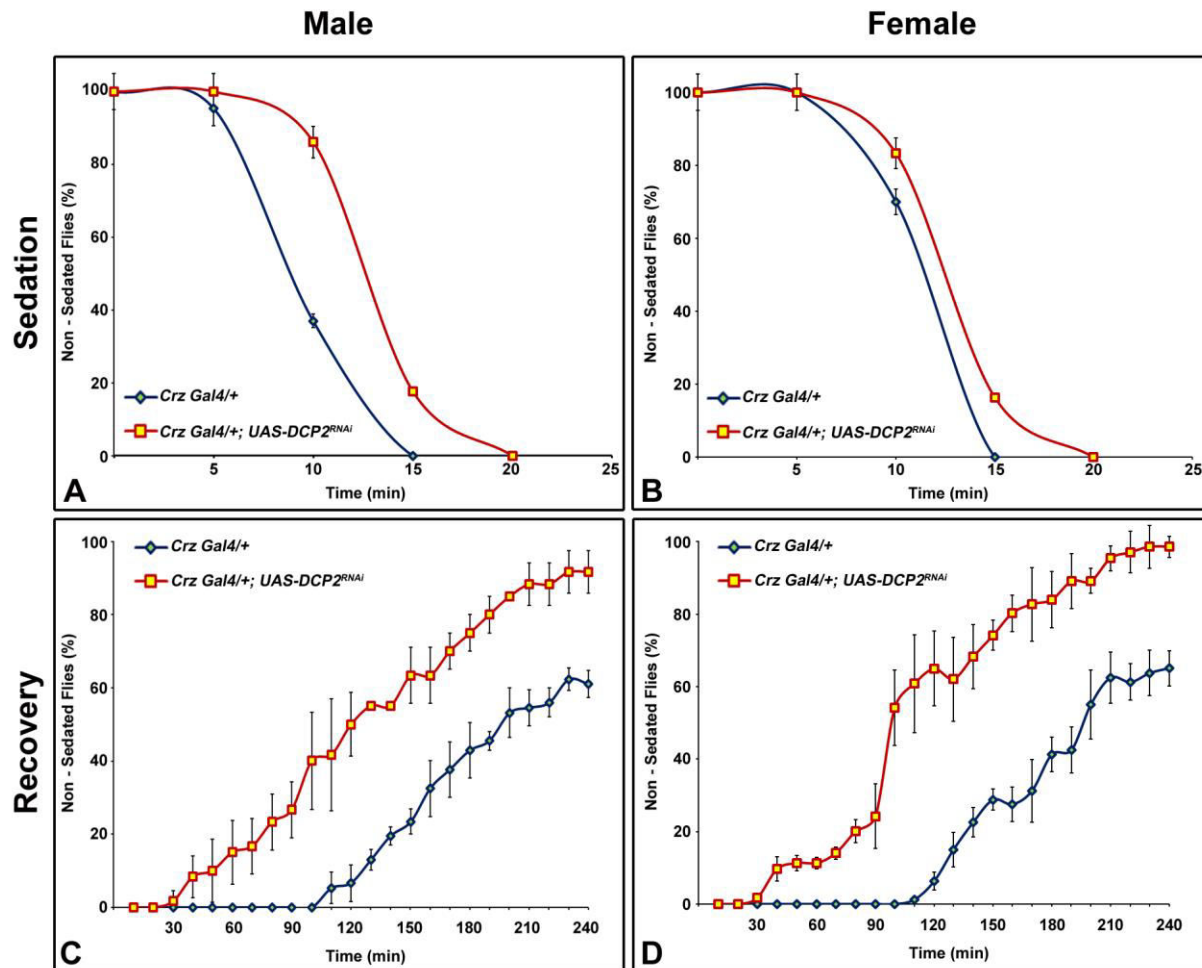
86



87

88 **Figure 13:** Mapping of the neuron(s) expressing DCP2 in the whole mount preparations of the larval
89 brain against the Corazonin expressing neurons. A-C shows the expression pattern of DCP2 and
90 Corazonin neurons in the larval brain. D-F and G-I show magnified view of the central brain and the
91 ventral ganglion respectively, where complete colocalization of DCP2 and Corazonin is visible.

92



93

94 **Figure 14:** Graphs showing the response to Ethanol induced sedation (A and B) in the control (*Crz-*
95 *Gal4/+*; blue lines) or *DCP2* knocked down (*Crz-Gal4/+; UAS-DCP2^{RNAi}/+*) flies (red lines) and
96 recovery from the same (C and D). The knocked-down flies (both male and female) show reduced
97 sensitivity to ethanol vapours as is visible from their delayed sedation behaviour (A and B) or enhanced
98 recovery from sedation (C and D).